

Inelastic scattering of microwave radiation in the dynamical Coulomb blockade

Juha Leppäkangas¹ and Michael Marthaler^{2,3}

¹*Physikalisches Institut, Karlsruhe Institute of Technology, 76131 Karlsruhe, Germany*

²*Institut für Theorie der Kondensierten Materie,
Karlsruhe Institute of Technology, 76131 Karlsruhe, Germany*

³*Theoretische Physik, Universität des Saarlandes, 66123 Saarbrücken, Germany*

We study scattering of propagating microwave fields by a DC-voltage biased Josephson junction. At sub-gap voltages, a small Josephson junction works merely as a non-linear boundary that can absorb, amplify, and diversely convert propagating microwaves. In the leading-order perturbation theory of the Josephson coupling energy, the spectral density and quadrature fluctuations of scattered thermal and coherent radiation can be described in terms of the well-known $P(E)$ function. Applying this, we study how thermal and coherent radiation is absorbed and amplified in an Ohmic transmission line and in a circuit with a resonance frequency. We show when a coherent input can create a two-mode squeezed output. In addition, we evaluate scattering amplitudes between arbitrary photon-number (Fock) states, characterizing individual photon multiplication and absorption processes occurring at the junction.

I. INTRODUCTION

Charge transport across a mesoscopic constriction is influenced by an interaction with its electromagnetic environment [1–7]. In earlier theoretical studies, the electromagnetic degrees of freedom have usually been traced out from the analysis, with a detailed focus on the mean electric current and its fluctuations. However, recent microwave-circuit experiments have demonstrated a simultaneous measurement of the current as well as various properties of the emitted and scattered microwave fields [8–21]. This technological progress has in turn sparked new theoretical efforts to better understand quantum properties of microwave radiation in mesoscopic transport [22–42]. Recent works have predicted and demonstrated effects such as microwave field squeezing [11, 25, 35, 37, 40, 41], photon-number multistability [23, 29], transmission blockade at certain photon number [33, 36], and creation of anti- or super-bunched microwave photons [18, 21, 22, 24, 30, 34]. In particular, a voltage-biased small Josephson junction has been utilized in applications providing microwave lasing [13, 17], parametric amplification [20], dispersive thermometry [15], and fast single-photon production [21].

In this article, we investigate theoretically how different forms of microwave fields scatter by a DC-voltage biased Josephson junction. We apply an input-output formalism of propagating radiation in a transmission line terminated by a Josephson junction [38, 43]. In the leading-order perturbation theory of the Josephson coupling energy, average spectral properties of scattered thermal and coherent fields can be described in terms of the $P(E)$ function [1, 2]. This function has earlier been used to characterize the average junction current [1, 2] and current fluctuations (microwave emission) [8, 24]. Here, we study its use in describing microwave scattering, accounting for an interaction between incoming radiation and junction current. We derive expressions for microwave absorption, amplification, and quadrature squeezing. In addition, we study scattering between indi-

vidual photon-number states (Fock states) and find that they are in the same perturbative limit determined by quadrature moments of a continuous-mode displacement operator.

Using the derived expressions, we investigate scattering of different forms of microwave fields in circuits with or without a resonance frequency. In particular, we investigate an interplay between thermal fluctuations and Cooper-pair shot noise in an Ohmic transmission line at low bias voltages. At higher bias voltages, we study how different types of radiation get absorbed or amplified [20] when biased close to a resonance condition. We also study when a coherent input can create a two-mode squeezed output. Furthermore, by applying the treatment based on calculating quadrature moments of a continuous-mode displacement operator, we characterize how incoming arbitrary photon-number in-states get converted into arbitrary photon-number out-states. The results allow for a straightforward analysis and engineering of arbitrary nonlinear processes in general electromagnetic environments.

The article is organized as follows. In Sec. II, we introduce the used input-output formalism and describe the treatment of various microwave fields as the input: Thermal radiation, coherent radiation, and Fock states. In Sec. III, we present general formulas describing absorption and conversion of thermal and coherent microwave fields in terms of the $P(E)$ function. We study absorption and amplification of low- and high-frequency radiation at general bias voltages. In Sec. IV, we study quadrature fluctuations and squeezing of the created output when having a coherent input. In Sec. V, we study individual photon multiplication and absorption processes occurring at the junction by evaluating scattering-matrix elements between arbitrary Fock states. Conclusions and discussion are given in Sec. VI.

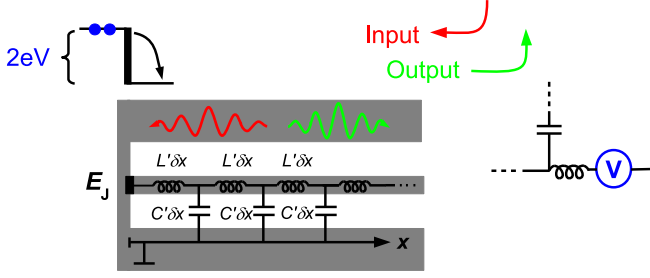


FIG. 1: We study scattering of propagating electromagnetic fields in a semi-infinite transmission line terminated by a Josephson junction with coupling energy E_J . In the dynamical Coulomb blockade regime, a voltage V is applied across the Josephson junction. Single-Cooper-pair transport is possible via emission of a photon at $2eV/\hbar$, or two (or more) photons at lower frequencies [2]. Incoming radiation of frequency ω can interact with Cooper-pair tunneling and, for example, trigger over-bias emission at $2eV/\hbar + \omega$.

II. THE SYSTEM AND THE MODEL

The microwave circuit we consider is shown in Fig. 1. It consists of a DC-voltage biased superconducting transmission line terminated by a Josephson junction with coupling energy E_J and critical current $I_c = (2e/\hbar)E_J$. In an experimental realization [8], the system can be DC biased via a low-pass filter (inductor) as high-frequency microwave photons propagate and are measured via a high-pass filter (capacitor), see Fig. 1. In the used continuous-mode treatment, the transmission line is described by a semi-infinite lumped-element circuit terminated by the (non-linear) Josephson inductance. We consider mostly explicitly an Ohmic transmission line, i.e., a constant inductance L' and capacitance C' per unit length, but the following analysis can be generalized to setups with resonance frequencies [38].

A. Hamiltonian

A starting point is the system Hamiltonian [38]

$$H = H_{EE} + H_J. \quad (1)$$

Here H_{EE} describes the electromagnetic environment, in this case the transmission line including the junction capacitor, and H_J describes Cooper-pair tunneling across the Josephson junction at the end of the transmission line. The combined Hamiltonian of the junction capacitor and of the semi-infinite transmission line has the form

$$H_{EE} = \frac{\hat{Q}^2}{2C} + \sum_{n=1}^{\infty} \left[\frac{\hat{q}_n^2}{2C'\delta x} + \frac{1}{2L'\delta x} (\hat{\Phi}_n - \hat{\Phi}_{n-1})^2 \right]. \quad (2)$$

This is a sum of inductive (L') and capacitive (C') energies per infinitesimal length δx , enumerated according to nodes (islands) on the central conductor, and

added with the charging energy of the junction capacitor C . The fluxes and charges at each node satisfy $[\hat{\Phi}_n, \hat{q}_m] = 2ie\delta_{mn}$, with $\hat{\Phi}_0$ being the flux and $\hat{Q} = \hat{q}_0$ the charge at the Josephson junction. Other combinations of the commutators are zero. The Cooper-pair tunneling across the Josephson junction is described by the Hamiltonian

$$H_J = -E_J \cos \left(\omega_J t - \frac{2e\hat{\Phi}_0}{\hbar} \right). \quad (3)$$

Here $\omega_J = 2eV/\hbar$ accounts for the DC-voltage bias.

In the following, we mark $\hat{\phi} \equiv (2e/\hbar)\hat{\Phi}_0$, which corresponds to the superconducting phase difference across the Josephson junction, relative to the applied DC-voltage V .

B. Input-output formalism

In the limit of vanishing node length, $\delta x \rightarrow 0$, the Heisenberg equations of motion for the magnetic fluxes at each node convert into a Klein-Gordon wave equation

$$\ddot{\hat{\Phi}}(x, t) = \frac{1}{L_i C_i} \frac{\partial^2 \hat{\Phi}(x, t)}{\partial^2 x}. \quad (4)$$

Here $\hat{\Phi}(x, t)$ is the position-dependent magnetic-flux field operator. The solution is a propagating electromagnetic field in the transmission line ($x > 0$), which we write in the form

$$\hat{\Phi}(x, t) = \sqrt{\frac{\hbar Z_0}{4\pi}} \int_0^\infty \frac{d\omega}{\sqrt{\omega}} \times \left[\hat{a}_{\text{in}}(\omega) e^{-i(k_\omega x + \omega t)} + \hat{a}_{\text{out}}(\omega) e^{-i(-k_\omega x + \omega t)} + \text{H.c.} \right]. \quad (5)$$

The creation operators of the incoming photons, $\hat{a}_{\text{in}}^\dagger(\omega)$, and the corresponding annihilation operators, $\hat{a}_{\text{in}}(\omega)$, satisfy

$$[\hat{a}_{\text{in}}(\omega), \hat{a}_{\text{in}}^\dagger(\omega')] = \delta(\omega - \omega'). \quad (6)$$

In a consistent solution, this relation is also valid for the operators of the out-field. This has been shown explicitly to hold at least up to second-order in E_J in Ref. [43]. The wave number $k_\omega = \omega\sqrt{C'L'}$ and the characteristic impedance $Z_0 = \sqrt{L'/C'}$.

At the Josephson junction ($x = 0$) the interaction between the electromagnetic radiation and Cooper-pair tunneling is described by the boundary condition

$$C\ddot{\hat{\Phi}}(0, t) - \frac{1}{L'} \frac{\partial \hat{\Phi}(x, t)}{\partial x} \Big|_{x=0} = I_c \sin \left[\omega_J t - \hat{\phi}(t) \right]. \quad (7)$$

The boundary condition manifests the Kirchhoff's rule for current conservation at the end of the semi-infinite transmission line.

C. Input states

In this article, we consider incoming microwave radiation of the following forms: (i) thermal radiation, (ii) stationary coherent radiation with a thermal background, and (iii) a single- or multi-photon pulse. Consider first the treatment of a deterministic coherent signal at frequency ω_0 . At zero temperature such state is constructed as [44]

$$|\text{in}\rangle = \hat{D}|0\rangle \equiv |\alpha\rangle. \quad (8)$$

Here $|0\rangle$ stands for the continuous-mode vacuum and \hat{D} is a displacement operator defined as

$$\hat{D} = \exp \left[\alpha^* \hat{a}_{\text{in}}^\dagger(\omega_0) - \alpha \hat{a}_{\text{in}}(\omega_0) \right]. \quad (9)$$

This satisfies

$$\hat{D}^\dagger \hat{D} = 1. \quad (10)$$

Using the notation $\alpha = \sqrt{2\pi F} e^{i\theta}$, the state gives for the correlation function

$$\langle \hat{a}_{\text{in}}^\dagger(\omega) \hat{a}_{\text{in}}(\omega') \rangle = 2\pi F \delta(\omega - \omega_0) \delta(\omega' - \omega). \quad (11)$$

The photon flux density of the incoming radiation is defined as [44]

$$f_{\text{in}}(\omega) \equiv \frac{1}{2\pi} \int d\omega' \langle \hat{a}_{\text{in}}^\dagger(\omega) \hat{a}_{\text{in}}(\omega') \rangle = F \delta(\omega - \omega_0). \quad (12)$$

The total incoming photon flux is then F .

We will now account for thermal radiation at lower frequencies, considering still the case (ii). In this article, we assume $\omega_0 \gg k_B T / \hbar$, so that thermal photons do not practically exist at the drive frequency ω_0 . Furthermore, the statistics of thermal radiation is probabilistic: We need to introduce a (formal) density operator $\hat{\rho}$. We state that the statistics of incoming radiation is described by

$$\hat{\rho} = \hat{D} \hat{\rho}_{\text{th}} \hat{D}^\dagger, \quad (13)$$

where $\hat{\rho}_{\text{th}}$ describes bare thermal distribution. This state gives for the correlation function

$$\begin{aligned} \langle \hat{a}_{\text{in}}^\dagger(\omega) \hat{a}_{\text{in}}(\omega') \rangle &= \frac{1}{e^{\beta \hbar \omega} - 1} \delta(\omega - \omega') \\ &+ 2\pi F \delta(\omega - \omega_0) \delta(\omega' - \omega). \end{aligned} \quad (14)$$

The limit $F = 0$ ($\hat{D} = 1$), then corresponds to the case of a bare thermal input, i.e., case (i).

Finally, in the case of a single-photon input, we have a deterministic input state (pulse)

$$|\text{in}\rangle = \hat{a}_\xi^\dagger |0\rangle = \int_0^\infty d\omega \xi(\omega) \hat{a}_{\text{in}}^\dagger(\omega) |0\rangle. \quad (15)$$

Here $\xi(\omega)$ describes the waveform of the incoming photon with normalization $\int_0^\infty d\omega |\xi(\omega)|^2 = 1$. The finite width is needed since any finite photon-number field has a form of a pulse [44]. Using Eq. (6) one can show that such single-photon creation and annihilation operators satisfy

$$[\hat{a}_\xi, \hat{a}_\xi^\dagger] = 1. \quad (16)$$

Multi-photon states are created analogously.

D. Solution

In the input-output theory, the solution of the out field can be expressed as a function of the time evolution at the boundary [45]. In our problem, the the out field becomes a function of the junction current I_J [38],

$$\begin{aligned} \hat{a}_{\text{out}}(\omega) &= \hat{a}_0(\omega) + i \sqrt{\frac{Z_0}{\pi \hbar \omega}} A(\omega) \int_{-\infty}^\infty dt e^{i\omega t} \\ &\times \hat{U}^\dagger(t, -\infty) \hat{I}_J^0(t) \hat{U}(t, -\infty). \end{aligned} \quad (17)$$

Here the zeroth-order out-operator has the form

$$\hat{a}_0(\omega) = \frac{A(\omega)}{A^*(\omega)} \hat{a}_{\text{in}}(\omega), \quad (18)$$

where the function $A(\omega)$ accounts for the surrounding linear microwave circuit, for an Ohmic transmission having the form

$$A(\omega) = \frac{1}{1 - i\omega Z_0 C}. \quad (19)$$

This function can also incorporate reflections (resonances) in the transmission line [38]. The free-evolution solution ($E_J = 0$) for the junction current is

$$\hat{I}_J^0(t) = I_c \sin [\omega_J t - \hat{\phi}_0(t)], \quad (20)$$

and the time-evolution is defined by the operator [46]

$$\hat{U}(t, t_0) = \mathcal{T} \exp \left\{ \frac{i}{\hbar} \int_{t_0}^t dt' H_J^0(t') \right\}, \quad (21)$$

where \mathcal{T} is the time-ordering operator. This provides a series expansion of system quantities in powers of the Josephson coupling. The phase difference across the Josephson junction has a zeroth-order solution [2, 43]

$$\hat{\phi}_0(t) = \frac{\sqrt{4\pi \hbar Z_0}}{\Phi_0} \int_0^\infty \frac{d\omega}{\sqrt{\omega}} A(\omega) a_{\text{in}}(\omega) e^{-i\omega t} + \text{H.c.} \quad (22)$$

The first- and second-order solutions for the out-field operator $\hat{a}_{\text{out}}(\omega)$ are written down explicitly in Appendix A.

E. Phase fluctuations

In the evaluation of the spectral density and quadrature fluctuations of the out-field, a central quantity is the function

$$P(t, t') \equiv \left\langle e^{i\hat{\phi}_0(t)} e^{-i\hat{\phi}_0(t')} \right\rangle. \quad (23)$$

This connects Cooper-pair tunneling to the spectral structure of the electromagnetic environment [1, 2]. The explicit form of this ensemble average depends on the input field. Let us shortly consider the form of this function in the cases of thermal and coherent inputs.

In thermal equilibrium, the free-evolution phase fluctuations satisfy [2]

$$P_{\text{th}}(t, t') = e^{J_{\text{th}}(t-t')}, \quad (24)$$

where the phase-correlation function has the form

$$J_{\text{th}}(t) = \left\langle \left[\hat{\phi}_0(t) - \hat{\phi}_0(0) \right] \hat{\phi}_0(0) \right\rangle_{\text{th}}. \quad (25)$$

Using Eqs. (14) and (22) one obtains

$$\left\langle \hat{\phi}_0(t) \hat{\phi}_0(t') \right\rangle_{\text{th}} = 2 \int_{-\infty}^{\infty} \frac{d\omega}{\omega} \frac{\text{Re}[Z_t(\omega)]}{R_Q} \frac{e^{-i\omega(t-t')}}{1 - e^{-\beta\hbar\omega}}. \quad (26)$$

Here $R_Q = h/4e^2$ is the superconducting resistance quantum and we have defined the (real part of the) tunnel impedance as [2, 38]

$$\text{Re}[Z_t(\omega)] = Z_0 |A(\omega)|^2. \quad (27)$$

Note that the quantity $J_{\text{th}}(t)$ is a complex valued function, accounting for vacuum fluctuations.

In the case of the coherent-state input we can use the property [44]

$$\hat{D}^\dagger \hat{a}^{(\dagger)}(\omega) \hat{D} = \hat{a}^{(\dagger)}(\omega) + \alpha^{(*)} \delta(\omega - \omega_0). \quad (28)$$

It follows that

$$\hat{D}^\dagger \hat{I}_J^0(t) \hat{D} = I_c \sin \left[\omega_J t - \hat{\phi}_0(t) - \phi_{\omega_0}(t) \right], \quad (29)$$

where

$$\phi_{\omega_0}(t) = \frac{\sqrt{4\pi\hbar Z_0}}{\Phi_0} \frac{A(\omega_0)}{\sqrt{\omega_0}} \alpha e^{-i\omega_0 t} + \text{H.c.} \quad (30)$$

Also the time-evolution operator transforms similarly since

$$\hat{D}^\dagger H_J^0(t) \hat{D} = -E_J \cos \left[\omega_J t - \hat{\phi}_0(t) - \phi_{\omega_0}(t) \right]. \quad (31)$$

It follows that the effect of incoming coherent radiation can be accounted for by adding an AC-component to the applied voltage V . We then get for the relevant phase-

fluctuation function

$$P_{\text{coh}}(t, t') = e^{i\phi_{\omega_0}(t)} e^{-i\phi_{\omega_0}(t')} e^{J_{\text{th}}(t-t')}. \quad (32)$$

Furthermore, if we assume that $A(\omega_0)\alpha$ is a real number, the additional phase due to the incoming coherent signal has the form

$$\phi_{\omega_0}(t) = a \cos \omega_0 t, \quad (33)$$

where a is a real number

$$a = \sqrt{\frac{8Z_0}{\omega_0 R_Q}} \alpha A(\omega_0). \quad (34)$$

III. SCATTERING OF THERMAL AND COHERENT RADIATION

In this section, we investigate scattering of thermal and coherent microwave radiation. The results are obtained by a leading-order expansion in the critical current I_c . The technical calculation involves time integrations of quantities similar to phase-fluctuation function $P(t, t')$, Eq. (23), and is detailed in Appendix A. An energy conservation of the theory is proven in Appendix B.

We start by presenting general formulas for the photon flux density and power spectral density, describing changes between the incoming and outgoing microwave fields at certain frequencies. After this, we analyze more detailed specific phenomena predicted by these formulas, namely conversion and absorption of thermal radiation at low-frequencies and amplification of coherent signals at high frequencies. Quadrature squeezing of the outgoing field will be studied in Sec. IV. Simultaneous dispersive shift in the reflected field has been investigated theoretically and experimentally in Ref. [15].

A. General formulas

The photon flux density of propagating fields in the transmission line is defined as [44]

$$f_{\text{in/out}}(\omega) = \frac{1}{2\pi} \int d\omega' \left\langle \hat{a}_{\text{in/out}}^\dagger(\omega') \hat{a}_{\text{in/out}}(\omega) \right\rangle, \quad (35)$$

and the equivalent power density accounts for the single-photon energy $\hbar\omega$ and is

$$\mathcal{P}_{\text{in/out}}(\omega) = \hbar\omega f_{\text{in/out}}(\omega). \quad (36)$$

In the following, we present the total result using different contributions in the form

$$f_{\text{out}}(\omega) - f_{\text{in}}(\omega) = f_{\text{em}}(\omega) - f_{\text{abs}}(\omega). \quad (37)$$

The left-hand side then considers the difference between incoming and outgoing photon fluxes and the right-hand

side separates between inelastic contributions where new radiation is created (em) and incoming radiation is absorbed (abs). The term $f_{\text{in}}(\omega)$ corresponds to the result for $E_J = 0$ and is determined by Eq. (14).

1. Emission and absorption

The function $f_{\text{em}}(\omega) \geq 0$ describes how radiation is emitted by the junction current fluctuations. The contribution can be expressed as

$$f_{\text{em}}(\omega) = \frac{1}{1 - e^{-\beta\hbar\omega}} \frac{I_c^2 \text{Re}[Z_t(\omega)]}{2\omega} \quad (38)$$

$$\times \sum_{\pm} \sum_{n=-\infty}^{\infty} P[\hbar(\pm\omega_J + n\omega_0 - \omega)] |J_n(a)|^2$$

$$+ \delta(\omega - \omega_0) \frac{I_c^2 R_Q}{4} \sum_{\pm} \sum_{n=1}^{\infty} |J_n(a)|^2 n P[\hbar(\pm\omega_J - n\omega_0)] .$$

This is a function of the probability distribution $P(E)$ [1, 2], defined as the Fourier transform of the phase correlation function of the thermal field, Eq. (24),

$$P(E) = \frac{1}{2\pi\hbar} \int_{-\infty}^{\infty} dt \left\langle e^{i\hat{\phi}_0(t)} e^{-i\hat{\phi}_0(0)} \right\rangle_{\text{th}} e^{i\frac{E}{\hbar}t}$$

$$= \frac{1}{2\pi\hbar} \int_{-\infty}^{\infty} dt e^{J_{\text{th}}(t) + i\frac{E}{\hbar}t} , \quad (39)$$

Here, the plus (minus) sign in front of ω_J corresponds to contribution from forward (backward) Cooper-pair tunneling. Since the result for bare thermal radiation corresponds to $a = 0$, we see that for a finite amplitude a , sidebands appear to the emission spectrum, separated by multiples of the drive frequency ω_0 . The summation over n then corresponds to a number of photons exchanged with the drive field in a tunneling process. The extra contribution at frequency ω_0 [the bottom line of Eq. (38)] describes emission in the drive mode.

The result for the function $f_{\text{abs}}(\omega) \geq 0$ is analogous. It describes how radiation is absorbed by the junction current fluctuations and has the form

$$f_{\text{abs}}(\omega) = \frac{1}{e^{\beta\hbar\omega} - 1} \frac{I_c^2 \text{Re}[Z_t(\omega)]}{2\omega} \quad (40)$$

$$\times \sum_{\pm} \sum_{n=-\infty}^{\infty} P[\hbar(\pm\omega_J + n\omega_0 + \omega)] |J_n(a)|^2$$

$$+ \delta(\omega - \omega_0) \frac{I_c^2 R_Q}{4} \sum_{\pm} \sum_{n=1}^{\infty} |J_n(a)|^2 n P[\hbar(\pm\omega_J + n\omega_0)] .$$

Here, again, the plus (minus) sign in front of ω_J corresponds to contribution from forward (backward) Cooper-pair tunneling and the summation over n then corresponds to a number of photons exchanged with the drive field in a tunneling process. The extra contribution at frequency ω_0 describes the effect of such absorption to

the drive mode.

The functions f_{em} and f_{abs} are related by the transformation $\omega \rightarrow -\omega$ and $n \rightarrow -n$, reflecting that emission and absorption are in a quantum theory connected by a sign change in the Fourier transformation of a noise correlation function.

2. Junction current fluctuations

In earlier works, a direct connection between the $P(E)$ theory and junction current fluctuations has been established [8, 24, 38]

$$\left\langle \hat{I}_J(t) \hat{I}_J(0) \right\rangle_{\omega} \quad (41)$$

$$= \pi \hbar \frac{I_c^2}{2} \sum_{\pm} \sum_{n=-\infty}^{\infty} P[\hbar(\pm\omega_J - n\omega_0 - \omega)] |J_n(a)|^2 ,$$

This differs from f_{em} by not having $(1 - e^{-\beta\hbar\omega})^{-1}$ and $\text{Re}[Z_t(\omega)]$ as front factors. In the zero-temperature limit, the power density of the emitted radiation is then, up to a frequency-dependent front factor, the finite-frequency current noise of the Josephson current [38]. At finite temperatures, however, this is not the total spectrum of out-radiation, since the formula based only on the current fluctuations does not correctly account for changes in the input field. This becomes evident, for example, when looking the contribution at coherent drive frequencies (delta-function contributions), which are missing in the current correlator. In an exactly similar way, the absorption of (and the induced emission to) the thermal field is not included. This difference is studied further below.

B. Low-frequency phenomena

1. Disappearance of the junction at $V = 0$

An illustrative example of changes between incoming and outgoing fields is the case of zero voltage bias, $V = 0$, and the absence of coherent drive, $a = 0$. Here, the power supplied by the voltage source vanishes, $IV = 0$, so no changes in the total power is expected. We can indeed use the detailed balance symmetry of the $P(E)$ function [2], $P(-E) = e^{-\beta E} P(E)$, to show that in this case

$$f_{\text{em}}(\omega) - f_{\text{abs}}(\omega) = 0 . \quad (42)$$

Thus, an undriven and unbiased Josephson junction does not modify the thermal radiation at all: The outgoing radiation is still thermal and exactly of the same form as the input radiation. This result is seen in Fig. 2(b), as the 'avoided crossing' emerging at $2eV/\hbar = 0$, in comparison to the diagonal Josephson AC-current line in Fig. 2(a).

For higher DC voltages an additional zero-frequency

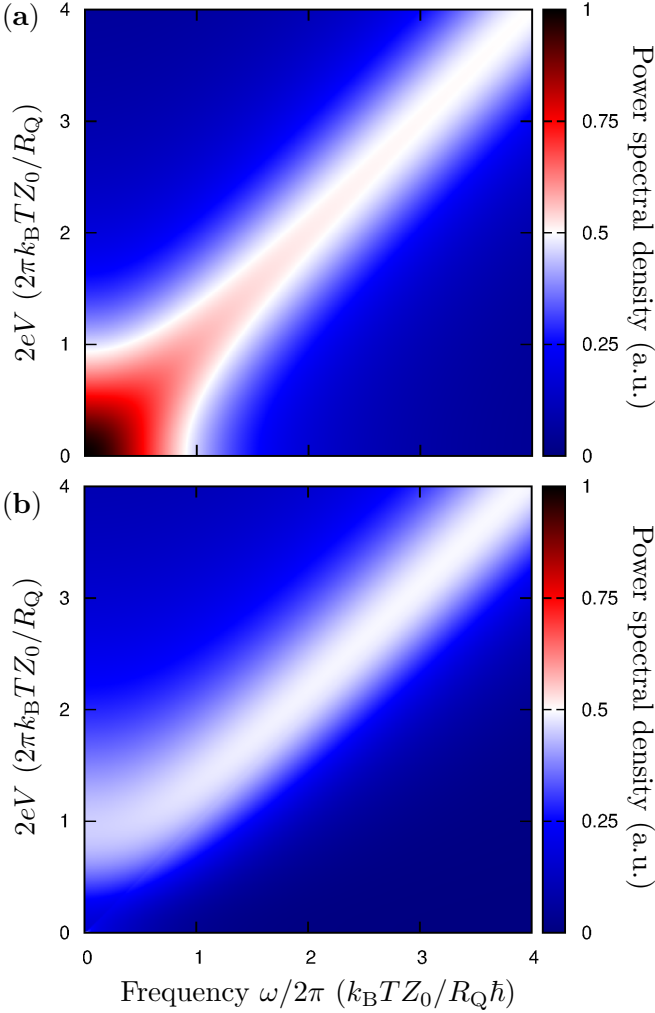


FIG. 2: (a) Power spectral density of junction current fluctuations, $\langle \hat{I}_J(t) \hat{I}_J(0) \rangle_\omega$, of a Josephson junction terminating a voltage V biased Ohmic transmission line with a thermal input. The current fluctuations occur predominantly at the diagonal line, corresponding to Josephson frequency $\omega_J = 2eV/\hbar$. (b) The simultaneous change in the power density, $\mathcal{P}_{\text{out}}(\omega) - \mathcal{P}_{\text{in}}(\omega)$. The 'bending' and disappearance of the added power at $2eV/\hbar = 0$ manifests that at zero bias the Josephson junction does not modify the spectrum of the propagating thermal field. For a finite voltage bias a local maximum of added (zero-frequency) noise appears at $2eV \approx 2\pi k_B T Z_0 / R_Q$. The parameters are $Z_0 = 100 \, \Omega$, $C_J = 100 \, \text{fF}$, and $T = 100 \, \text{mK}$.

noise appears. For low-Ohmic environments the noise has a maximum approximately at $2eV = 2\pi k_B T R_Q$, as seen in Fig. 2(b). This value corresponds to the width of the current-fluctuation spectrum at $\hbar\omega = 2eV$ [38]. At higher voltage-biases, the change in the power spectrum approaches the spectrum of the current correlator. Here, the additional out spectrum becomes a sum of a term

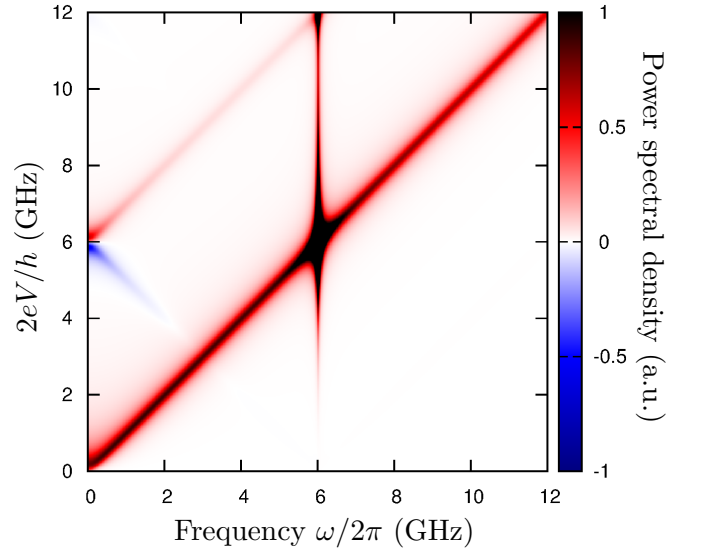


FIG. 3: Added power, $\mathcal{P}_{\text{out}}(\omega) - \mathcal{P}_{\text{in}}(\omega)$, by a voltage V biased Josephson junction in a transmission line with a resonance frequency at $\omega_r/2\pi = 6 \, \text{GHz}$ and incoming thermal radiation. Emission at the Josephson frequency (at the diagonal line) is enhanced close to the resonance frequency $2eV/\hbar = \omega_r$. In particular, when biased just below the resonance frequency, $2eV/\hbar \lesssim \omega_r$, emission to the resonance frequency absorbs incoming thermal radiation (blue region at low frequencies). Vice versa, when biased just above the resonance frequency, emission to the resonance frequency increases low-frequency radiation. The parameters are $Z_0 = 100 \, \Omega$, $C_J = 100 \, \text{fF}$, and $T = 100 \, \text{mK}$. The impedance $\text{Re}[Z_t(\omega)]$ is added by a Lorentzian corresponding to a $\omega_r/2\pi = 6 \, \text{GHz}$ resonator with quality factor 100 and characteristic impedance $Z_{LC} = 100 \, \Omega$.

proportional to $\langle \hat{I}_J(t) \hat{I}_J(0) \rangle_\omega$ and a term

$$\frac{1}{e^{\beta\hbar\omega} - 1} \frac{\hbar I_c^2 \text{Re}[Z_t(\omega)]}{2} \times [P(2eV - \hbar\omega) - P(2eV + \hbar\omega)]. \quad (43)$$

In the limit $\omega \rightarrow 0$, this additional contribution becomes proportional to $k_B T \partial P(E) / \partial E|_{E=2eV}$. This needs to be compared to $P(2eV)$, the magnitude of $\langle I_J(t) I_J(0) \rangle_{\omega=0}$. For a low-Ohmic transmission line, and in the limit $E \gg k_B T$, we have $P(E) \sim Z_0 / R_Q E$. This means that for $k_B T / 2eV < 1$ the correction to the low-frequency noise is dominated by the shot noise in the junction current, as also seen in Fig. 2 by the similarity of the two spectral densities at high bias voltages. Such interplay between transport noise and thermal fluctuations in the power spectrum has been analyzed recently also in Ref. [47].

2. Low-frequency absorption in a resonance circuit

Absorption of radiation occurs when the contribution $f_{\text{em}}(\omega) - f_{\text{abs}}(\omega)$ is negative. Such a result is sound as long as the total flux, $f_{\text{out}}(\omega) = f_{\text{in}}(\omega) + f_{\text{em}}(\omega) - f_{\text{abs}}(\omega)$,

is positive, which is always possible for small enough coupling energy E_J .

We obtain that photon-assisted tunneling absorbs thermal energy generally if

$$P(2eV - \hbar\omega) + \frac{1}{e\beta\hbar\omega - 1} [P(2eV - \hbar\omega) - P(2eV + \hbar\omega)] < 0. \quad (44)$$

Multiplying the left-hand side expression by $\hbar I_c^2 \text{Re}[Z_t(\omega)]/2$ one obtains the absorption power density. Here, the interpretation is that Cooper-pair tunneling extracts thermal radiation as described by the term $P(2eV + \hbar\omega)$, emits new radiation induced by thermal radiation field, the middle term $P(2eV - \hbar\omega)$, and emits new radiation induced by vacuum fluctuations, the first term $P(2eV - \hbar\omega)$.

The cooling effect can occur, for example, in a circuit with resonance frequency $\omega_r \gg k_B T/\hbar$ when voltage biased below the single-photon emission resonance $\omega_J \lesssim \omega_r$. Here, thermal-photon assisted Cooper-pair tunneling, with emission to the resonance frequency, is favored. This cooling effect is seen as the blue region in Fig. 3, where we consider a circuit with a resonance frequency at 6 GHz. This effect works also vice versa: Biasing just above heats the environment. It is possible to use thermal-photon assisted tunneling to cool electromagnetic degrees of freedom of quantum microwave devices [16, 48].

C. Drive field amplification

We study now amplification and absorption of a coherent input at frequency ω_0 , i.e., flux changes in Eqs. (38) and (40) as given by the delta-function contributions. This can be characterized by a gain function

$$G = \frac{f_{\text{out}}(\omega_0)}{f_{\text{in}}(\omega_0)} - 1 = \frac{4\pi I_c^2 \text{Re}[Z_t(\omega_0)]}{\omega_0} \times \frac{\sum_{\pm} \sum_{n=-\infty}^{\infty} |J_n(a)|^2 n P[\hbar(\pm\omega_J - n\omega_0)]}{a^2} - 1. \quad (45)$$

A positive (negative) value of G corresponds to an increase (decrease) of the drive-mode photon flux. We assume an incoming coherent state $|\alpha\rangle$ with photon flux $|\alpha|^2/2\pi$ and parameter a is obtained by using connection (34).

Two competing effects appear when $\omega_J \sim \omega_0$. If the voltage is tuned above the drive, $\omega_J \gtrsim \omega_0$, induced emission to the drive frequency can occur through forward Cooper-pair tunneling and additional photon emission to $\omega_J - \omega_0$ (or multiphoton emission dissipating the rest energy $\hbar\omega_J - \hbar\omega_0$). When voltage is tuned below the drive, $\omega_J \lesssim \omega_0$, drive photons can be absorbed through backward Cooper-pair tunneling and photon emission to $\omega_0 - \omega_J$ (or multiphoton emission dissipating the rest energy $\hbar\omega_0 - \hbar\omega_J$). On resonance $\omega_J = \omega_0$, these

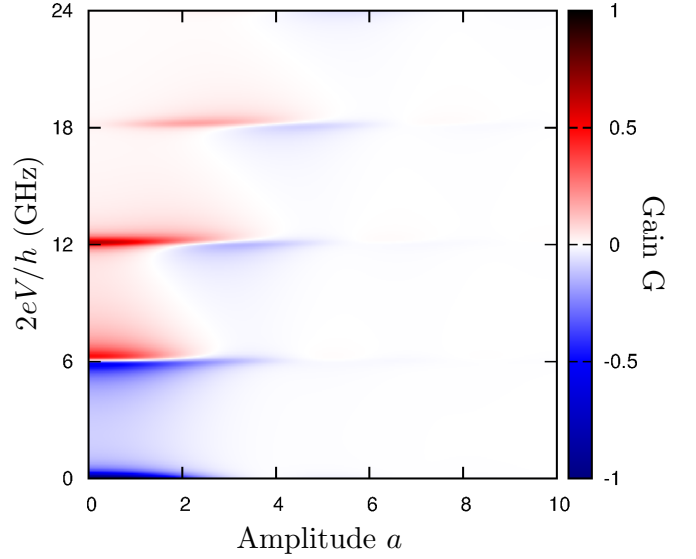


FIG. 4: Gain of incoming photon flux for different drive amplitudes a and bias voltages V , as defined by Eq. (45). We consider a coherent input at $\omega_0/2\pi = 6$ GHz and a system as in Fig. 3. Depending on the voltage bias, Cooper-pair tunneling can increase or decrease the flux of photons at ω_0 . In particular, just above $2eV/\hbar = \omega_0$ (and $a \lesssim 2$), induced emission to the drive beam occurs through forward Cooper-pair tunneling and low-frequency photon emission. Just below $2eV/\hbar = \omega_0$, photons are absorbed from the drive beam through backward Cooper-pair tunneling and again low-frequency photon emission. The value of G is normalized here by $0.02\pi I_c^2 \text{Re}[Z(\omega_0)]/\hbar\omega_0 \text{GHz}$.

two effects cancel each other. The strength of this effect depends on the flux density at the drive frequency, $\sim \text{Re}[Z_t(\omega_0)]/\omega_0$, and on the probability to dissipate the rest energy, $P(\hbar|\omega_0 - \omega_J|)$. Similar processes are present also for multi-photon resonances $\omega_J \sim n\omega_r$, see Fig. 4. An experimental realization of this effect is demonstrated in Ref. [20], achieving near quantum-limited amplification of input signal.

D. Validity region of the perturbative approach and other possible approaches

In this article, we restrict to a leading-order perturbation theory in powers of the Josephson coupling energy E_J , or equivalently the critical current $I_c = (2e/\hbar)E_J$. We then implicitly assume the limit of weak interaction, where most of the input radiation is reflected, and this zeroth-order solution dominates when compared to the higher-order contributions.

A nonperturbative treatment in E_J in an electromagnetic environment consisting of two microwave resonators coupled weakly to transmission lines is presented in Ref. [49], where a deterministic photon multiplication is predicted. The present article then expands this analysis to account for arbitrary-shaped electromagnetic environ-

ments, with the restriction to the leading-order perturbation theory in the Josephson coupling energy.

IV. COHERENT INPUT: QUADRATURE SQUEEZED OUTPUT

Microwave radiation can scatter inelastically at a DC-voltage biased Josephson junction. In this section, we investigate quadrature fluctuations of the created output in such processes. An electromagnetic field with quadrature fluctuations less than vacuum fluctuations is called quadrature squeezed and has numerous applications in quantum information and metrology [50].

A. Connection to previous works

Quadrature squeezed microwaves can be created in superconducting transmission lines in the presence of non-linear elements, provided, for example, by Josephson junctions [51–56]. They can also be emitted by quantum transport: Inelastic Cooper-pair tunneling produces nonclassical photon pairs below the classical Josephson radiation peak [18, 24, 31], and this radiation is ideally quadrature squeezed [25]. However, as being sensitive to junction phase fluctuations, squeezing with respect to a fixed angle is washed out in a dephasing time that is in typical experimental conditions less than a microsecond [43], which however can be increased by careful engineering of the low-frequency impedance.

In this section, we find a production of photon pairs and quadrature squeezing by a different process. This includes two opposite-direction Cooper-pair tunneling events and splitting of one drive photon of frequency ω_0 , Fig. 5(b). Such production is thereby robust against low-frequency voltage fluctuations, since the total energy of the two photons does not depend on the bias voltage. An analogous phenomenon has been recently predicted [35, 37, 41] and measured [11] in driven conductors taking use of quasiparticle excitations.

B. Definition of quadrature squeezing for continuous-mode fields

For this analysis we need a careful definition of quadrature squeezing for continuous-mode fields [44]. We study fluctuations of a field operator

$$\hat{O} = \int_{\text{BW}} d\omega \left[\hat{a}(\omega) e^{-i\theta(\omega)} + \hat{a}^\dagger(\omega) e^{+i\theta(\omega)} \right]. \quad (46)$$

Here BW stands for the detector bandwidth, in general introducing a detector filter function [38, 57], in the simplest case just implying integration between two frequencies. The variable $\theta(\omega)$ corresponds to a continuous-mode

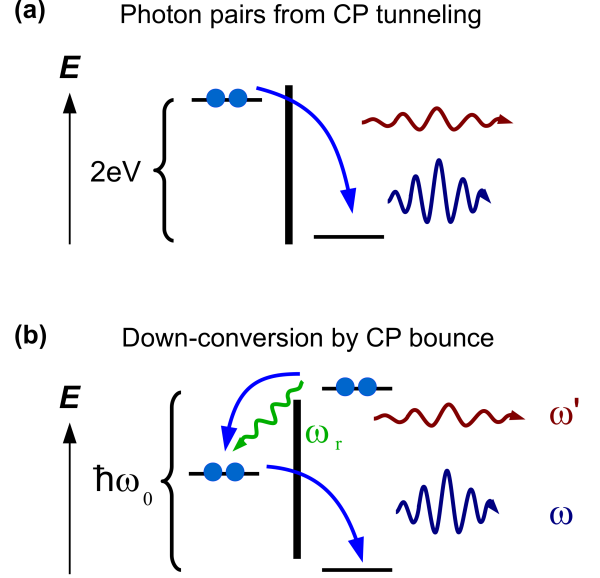


FIG. 5: Two ways to produce nonclassical photon pairs and quadrature squeezing by a DC-voltage biased Josephson junction. In case (a), two photons are created from the electrostatic energy released in a single Cooper-pair (CP) tunneling event. The process is similar to a parametric down conversion of a pump-field photon of frequency $\omega_J = 2eV/\hbar$. In case (b), correlated drive-photon assisted backward and forward CP tunneling events produce in total two outgoing photons, ω' and ω , whose frequencies sum up to the drive frequency ω_0 . In between a virtual photon of frequency ω_r is put (virtually) into the resonator and re-absorbed. Only process (b) is robust against low-frequency voltage fluctuations, since the total energy of the two outgoing photons does not depend on the fluctuating junction voltage. A drive-photon assisted single CP tunneling would be equivalent to process (a) and thereby affected by low-frequency fluctuations.

generalization of the considered quadrature angle. Fluctuations of this field are then characterized by the variance

$$\text{Var}[\hat{O}] \equiv \left\langle \left(\hat{O} - \langle \hat{O} \rangle \right)^2 \right\rangle = \langle \hat{O}^2 \rangle - \langle \hat{O} \rangle^2, \quad (47)$$

which can be written as

$$\text{Var}[\hat{O}] = \int_{\text{BW}} d\omega \int_{\text{BW}} d\omega' O(\omega, \omega'), \quad (48)$$

where

$$O(\omega, \omega') = \delta(\omega - \omega') + 2 \left\langle \hat{a}_1^\dagger(\omega) \hat{a}_1(\omega') \right\rangle + 2 \text{Re} \left[\left\langle \hat{a}_1(\omega) \hat{a}_1(\omega') \right\rangle e^{2i\theta(\omega)} \right]. \quad (49)$$

The first term on the right-hand side of Eq. (49) is the result for the vacuum, whose total contribution we mark

now as

$$\text{Var}[\hat{O}]_{\text{vac}} = \int_{\text{BW}} d\omega. \quad (50)$$

This is also (by definition) the minimum uncertainty of a classical field.

Consider then fluctuations of a squeezed state $\hat{D}_{\text{sq}}|0\rangle$, where the continuous-mode squeezing operator is defined as [44]

$$\hat{D}_{\text{sq}} = e^{\hat{P} - \hat{P}^\dagger} \quad (51)$$

$$\hat{P}^\dagger = \frac{1}{2} \int_0^{\omega_0} d\omega \beta(\omega) \hat{a}^\dagger(\omega) \hat{a}^\dagger(\omega_0 - \omega). \quad (52)$$

Here $\beta(\omega) = s(\omega)e^{iv(\omega)}$, with $s(\omega) > 0$, accounts for the frequency distribution of the radiation. It satisfies $\beta(\omega_0 - \omega) = \beta(\omega)$. This creates photon pair states symmetrically around the central frequency $\omega_0/2$. The corresponding photon flux density is

$$\langle \hat{a}^\dagger(\omega) \hat{a}(\omega') \rangle = \sinh^2[s(\omega)] \delta(\omega' - \omega). \quad (53)$$

The key property of a quadrature squeezed field is a finite value of the correlation function

$$\begin{aligned} \langle \hat{a}(\omega) \hat{a}(\omega') \rangle &= \cosh[s(\omega)] \sinh[s(\omega')] e^{iv(\omega')} \\ &\times \delta(\omega + \omega' - \omega_0). \end{aligned} \quad (54)$$

This leads to the variance

$$\begin{aligned} \text{Var}[\hat{O}] &= \text{Var}[\hat{O}]_{\text{vac}} + 2 \int_{\text{BW}} d\omega \sinh^2[s(\omega)] \\ &+ 2 \int_{\text{BW}} d\omega \cosh[s(\omega)] \sinh[s(\omega)] \cos[\theta(\omega) - v(\omega)]. \end{aligned} \quad (55)$$

In particular, the choices $\theta(\omega) = v(\omega)$ and $\theta(\omega) = v(\omega) + \pi$ give the maximal and minimal variances, respectively,

$$\text{Var}[\hat{O}] = \text{Var}[\hat{O}]_{\text{vac}} + \int_{\text{BW}} d\omega \{ \exp[\pm s(\omega)] - 1 \}, \quad (56)$$

where the plus (minus) sign corresponds to the maximum (minimum). Thus, for $s(\omega) \rightarrow \infty$ and $\theta(\omega) = v(\omega) + \pi$, the total variance approaches zero.

C. Quadrature squeezing in the dynamical Coulomb blockade

We now redo the calculation of Sec. IV B but now using the solution obtained for the scattered field, Eq. (17). We study fluctuations of the (outgoing) transmission-line voltage

$$\hat{V} = V_0 \int_{\text{BW}} d\omega \left[\sqrt{\omega} \hat{a}_{\text{out}}(\omega) e^{-i\theta(\omega)} + \sqrt{\omega} \hat{a}_{\text{out}}^\dagger(\omega) e^{+i\theta(\omega)} \right], \quad (57)$$

where $V_0 = \sqrt{\hbar Z_0/4\pi}$. The vacuum fluctuations are here then characterized by variance

$$\text{Var}[\hat{V}]_{\text{vac}} = V_0^2 \int_{\text{BW}} \omega d\omega. \quad (58)$$

Important is the magnitude of the diagonal correlator of type $\langle \hat{a}_{\text{out}}^\dagger(\omega) \hat{a}_{\text{out}}(\omega') \rangle$, which is the photon flux density. In the leading-order perturbation theory in powers of E_J this has the form

$$\begin{aligned} \omega \langle \hat{a}_{\text{out}}^\dagger(\omega) \hat{a}_{\text{out}}(\omega') \rangle &= \pi \delta(\omega - \omega') \\ &\times \sum_{n\pm} |J_n(a)|^2 I_c^2 Z_0 |A(\omega)|^2 P[\hbar(\pm\omega_J - n\omega_0 - \omega)]. \end{aligned} \quad (59)$$

We assume here $\omega, \omega' \gg k_B T/\hbar$ and $\omega, \omega' \neq \omega_0$. For the non-diagonal correlator we get (Appendix C)

$$\begin{aligned} \sqrt{\omega\omega'} \langle \hat{a}_{\text{out}}(\omega) \hat{a}_{\text{out}}(\omega') \rangle &= \pi I_c^2 Z_0 A(\omega) A(\omega') \times \\ &\sum_{n\pm} \pm i P[\hbar(\omega \mp \omega_J + n\omega_0)] J_n(a) J_{n+1}(a) \delta(\omega + \omega' - \omega_0). \end{aligned} \quad (60)$$

We consider here contributions with mode frequencies that sum to ω_0 . Unlike the photon flux density, this term can also be negative.

Using the simplified notation

$$\sqrt{Z(\omega)} \equiv \sqrt{Z_0 |A(\omega)|^2}, \quad (61)$$

we get a result for the variance

$$\begin{aligned} \text{Var}[\hat{V}] - \text{Var}[\hat{V}]_{\text{vac}} &= I_c^2 V_0^2 \int_{\text{BW}} d\omega \\ &\times \left[\sum_{n\pm} |J_n(a)|^2 Z(\omega) P[\hbar(\pm\omega_J + n\omega_0 - \omega)] + m \sum_{n\pm} J_n(a) J_{n+1}(a) \sqrt{Z(\omega)} \sqrt{Z(\omega_0 - \omega)} \{ \pm P[\hbar(\pm\omega_J + n\omega_0 + \omega)] \} \right]. \end{aligned} \quad (62)$$

We assume here that the integration range includes frequencies symmetrically around $\omega_0/2$ and the introduced

variable m is either -1 or 1 (see below). In the following, we call the integrand of this expression as the quadra-

ture fluctuation density. The left-hand side of Eq. (62) then compares the fluctuations of the out field to vacuum fluctuations. On the right-hand side we consider only the maximum values of the variance (as a function of squeezing angle θ), which leads to that the introduced variable m is either -1 or 1 (both of them can correspond to the minimum). We then find that in the leading-order perturbation theory also the quadrature fluctuations are described by the $P(E)$ -function, allowing for maximizing the effect by engineering the $P(E)$ -function.

Quadrature fluctuations with respect to vacuum fluctuations is visualized in Fig. 6(a) for an Ohmic transmission line and in Fig. 6(b) for a circuit with a resonance frequency. We plot here the integrand of Eq. (62) as a function of emission frequency ω and voltage V , when summed over the values at ω and $\omega' = \omega_0 - \omega$ (integration range is assumed to be symmetric around $\omega_0/2$). We find that for an Ohmic environment weak squeezing can occur for $\omega, \omega' \gtrsim 2eV/\hbar$, in a broadband region where the emission from forward Cooper-pair tunneling is minimized. For a resonance frequency at ω_r , on the other hand, we find that two-mode squeezing is strongly enhanced at a line $\hbar\omega = 2eV + \hbar\omega_r$ or equivalently at $\hbar(\omega_0 - \omega') = 2eV + \hbar\omega_r$, see Fig. 6(b). The interpretation is that at this line two-photon emission, to frequencies ω' and ω_r , occurs via drive-photon assisted backward tunneling, since now $\hbar(\omega' + \omega_r) = \hbar\omega_0 - 2eV$. This line also corresponds to the forward-tunneling process, where a photon from the resonator is absorbed to create a photon to frequency $\omega = 2eV/\hbar + \omega_r$. This combination of processes is visualized in Fig. 5(b). Another squeezing line we see in Fig. 6(b) is $\hbar\omega = -2eV + \hbar\omega_r$ or equivalently $\hbar(\omega_0 - \omega') = -2eV + \hbar\omega_r$. This correspond to the same processes as described above, but with reverse Cooper-pair tunneling directions. Note that squeezing does not occur at $\omega = \omega_r$.

In comparison to other works, we find that the oscillator state at frequency ω_r plays the same role as virtual population of quasiparticle states in the analogous effect in normal-state systems [11, 35, 37, 41]. Also in our system, no squeezing appears when $V = 0$. However, in a very similar setup, quadrature squeezing has been studied and measured in the framework of dynamical Casimir effect [52–54, 56]. Here, one has $V = 0$ but a large Josephson coupling energy E_J . In this situation, squeezing of the out field can indeed appear in long-time averages since the down-converted pairs have a fixed relative phase, provided by the "trapping" of the phase to a local minimum of the Josephson potential energy, $-E_J \cos \hat{\phi}$. This effect then occurs in the limit of large E_J .

V. SCATTERING OF FOCK STATES

In this section, we analyze how individual single- and multi-photon states scatter at a DC-voltage biased Josephson junction. We use here a different theoretic

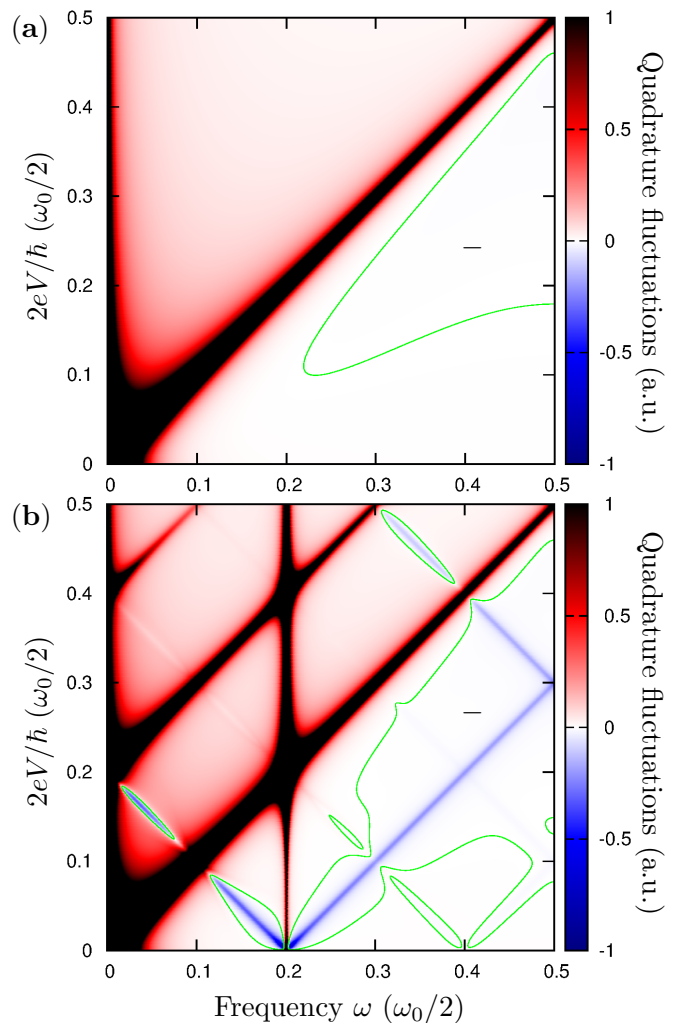


FIG. 6: Two-mode squeezing (negative values) between radiation frequencies ω and $\omega' = \omega_0 - \omega$ created by a coherently driven voltage V biased Josephson junction. We plot here the integrand of Eq. (62), when summed over frequencies ω and ω' . The coherent drive at ω_0 has an amplitude $a = 0.75$. (a) For an Ohmic transmission line, the variance can go below the vacuum level when $\omega, \omega' \gtrsim 2eV/\hbar$, where direct emission of photons from the voltage V is prohibited. This broadband region is indicated by the $-$ sign inside the contour line for vacuum fluctuations. (b) For a transmission line with a resonance frequency at $\omega_r = 0.2\omega_0$, two-mode squeezing occurs in the same region as for the Ohmic case, as well as in several other islands, surrounded by the vacuum-fluctuation level contour lines. Strong squeezing occurs at resonance lines corresponding to processes visualized in Fig. 5(b). The parameters are as in Fig. 3, but with $\omega_0/2\pi = 10$ GHz, $\omega_r/2\pi = 2$ GHz, $Z_{LC} = 700 \Omega$, and $T = 20$ mK.

cal formalism (than $P(E)$ theory): Rather than evaluating temporal changes in the photon flux density due to Fock-state pulses, a more informative approach here is

the evaluation of the scattering amplitudes

$$\begin{aligned} T^{1 \rightarrow n} &= T(\omega \rightarrow \omega_1 \dots \omega_n) \\ &= \left\langle [\hat{a}_{\text{out}}(\omega_1) \dots \hat{a}_{\text{out}}(\omega_n)] \hat{a}_{\text{in}}^\dagger(\omega) \right\rangle. \end{aligned} \quad (63)$$

The ensemble average is made with respect to vacuum state, which we mark as $|0\rangle$. This gives the amplitude for single incoming photon of frequency ω converting into n outgoing photons of frequencies $\omega_1, \dots, \omega_n$. The total amplitude for an incoming wavepacket is then an integration over individual frequencies with corresponding amplitudes: Integration over $\xi(\omega)$ in Eq. (15). Similarly for multi-photon inputs.

A. Output expressed using a continuous-mode displacement operator

We start this analysis by making a useful connection between the leading-order solution for the outgoing field and a continuous-mode displacement operator. For this we write the (zeroth-order) phase difference at the junction, Eq. (22), in the form

$$\begin{aligned} i\hat{\phi}_0(t) &= i \frac{\sqrt{4\pi\hbar Z_0}}{\Phi_0} \int_0^\infty \frac{d\omega}{\sqrt{\omega}} A(\omega) \hat{a}_{\text{in}}(\omega) e^{-i\omega t} - \text{H.c.} \\ &\equiv \hat{a}_\alpha - \hat{a}_\alpha^\dagger. \end{aligned} \quad (64)$$

Here, we have defined an unnormalized photon creation operator

$$\hat{a}_\alpha^\dagger = \int_0^\infty d\omega \alpha(\omega) e^{i\omega t} \hat{a}_{\text{in}}^\dagger(\omega) \quad (65)$$

$$\alpha(\omega) = -\frac{i}{\Phi_0} \sqrt{\frac{4\pi\hbar Z_0}{\omega}} A^*(\omega) = -i \sqrt{\frac{2Z_0}{R_Q \omega}} A^*(\omega). \quad (66)$$

For simplicity, we now neglect backward Cooper-pair tunneling, i.e., the term $\propto e^{i(\omega+\omega_J)t}$ in the leading-order solution of operator $\hat{a}_{\text{out}}(\omega)$ (Appendix A, $a = 0$). By using the definitions of Eqs. (64-66), we can then re-express the leading-order solution for the out-field operator as

$$\begin{aligned} \hat{a}_{\text{out}}(\omega) &= -\frac{\alpha^*(\omega)}{\alpha(\omega)} \hat{a}_{\text{in}}(\omega) \\ &+ \frac{I_c}{4e} \alpha^*(\omega) \int_{-\infty}^\infty dt e^{i(\omega-\omega_J)t} \exp[\hat{a}_\alpha - \hat{a}_\alpha^\dagger]. \end{aligned} \quad (67)$$

The out-field annihilation operator is now defined in terms of a continuous-mode displacement operator

$$\exp[\hat{a}_\alpha - \hat{a}_\alpha^\dagger] \equiv \hat{D}^\dagger(\alpha). \quad (68)$$

This connection originates from the form of the Josephson Hamiltonian ($\cos \hat{\phi}$ term), which in the quantized theory makes discrete shifts to the junction charge (Cooper-pair tunneling).

In the following, we exploit several important proper-

ties of a continuous-mode coherent state [44]

$$|\alpha(\omega)\rangle \equiv \hat{D}(\alpha)|0\rangle = \exp[\hat{a}_\alpha^\dagger - \hat{a}_\alpha]|0\rangle, \quad (69)$$

for which applies

$$\hat{a}_{\text{in}}(\omega)|\alpha(\omega)\rangle = \alpha(\omega) e^{i\omega t} |\alpha(\omega)\rangle \quad (70)$$

$$\langle 0|\alpha(\omega)\rangle = \exp\left[-\int d\omega |\alpha(\omega)|^2/2\right]. \quad (71)$$

The operator $\hat{D}(\alpha)$ itself satisfies

$$[\hat{a}_{\text{in}}(\omega), \hat{D}^{(\dagger)}(\alpha)] = (-)\alpha(\omega) e^{i\omega t} \hat{D}^{(\dagger)}(\alpha). \quad (72)$$

B. Evaluation of scattering amplitudes

Using the connection to the continuous-mode displacement operator, it is straightforward to evaluate general multi-photon scattering amplitudes to the leading order of critical current I_c . We write the general result in the form

$$T^{m \rightarrow n} = T_0^{m \rightarrow n} + T_1^{m \rightarrow n} + \dots \quad (73)$$

according to the order in the critical current I_c (or Josephson coupling energy $E_J = (\hbar/2e)I_c$).

1. Single-photon processes

Let us first consider the zeroth-order contribution T_0 . Using Eq. (67), we get (using $I_c = 0$)

$$T_0^{1 \rightarrow 1} = -\frac{\alpha^*(\omega_1)}{\alpha(\omega_1)} \left\langle \hat{a}_{\text{in}}(\omega_1) \hat{a}_{\text{in}}^\dagger(\omega) \right\rangle = -\frac{\alpha^*(\omega_1)}{\alpha(\omega_1)} \delta(\omega - \omega_1). \quad (74)$$

Here we used the relation $[\hat{a}_{\text{in}}(\omega), \hat{a}_{\text{in}}^\dagger(\omega')] = \delta(\omega - \omega')$ and that $\hat{a}_{\text{in}}|0\rangle = 0$. This element describes elastic scattering of an incoming photon. Such contribution exists only in the scattering between single-photon states, i.e., $T_0^{1 \rightarrow n} = 0$ for $n > 1$.

The leading-order contribution is obtained by using the term proportional to I_c in the out field, giving

$$\begin{aligned} T_1^{1 \rightarrow 1} &= \frac{I_c}{4e} \int_{-\infty}^\infty dt e^{i(\omega_1 - \omega_J)t} \alpha^*(\omega_1) \left\langle \hat{D}^\dagger(\alpha) \hat{a}_{\text{in}}^\dagger(\omega) \right\rangle \\ &= \frac{I_c}{4e} e^{-\bar{\rho}/2} \alpha^*(\omega) \alpha^*(\omega_1) 2\pi \delta(\omega_J + \omega - \omega_1), \end{aligned} \quad (75)$$

where we have used Eq. (70). This describes inelastic scattering of an incoming photon, where the electrostatic energy released in a Cooper-pair tunneling is absorbed, $\omega_1 = \omega + \omega_J$. The appearance of parameter

$$\bar{\rho} \equiv \int_0^\infty |\alpha(\omega)|^2 = \int_0^\infty \frac{d\omega}{\omega} \frac{2\text{Re}[Z_t(\omega)]}{R_Q} \quad (76)$$

follows from Eq. (71). [The expression as a function of tunnel impedance follows from Eqs. (66) and (27).]

The parameter $\tilde{\rho}$ corresponds to the average photon number of a coherent state $|\alpha(\omega)\rangle$,

$$\tilde{\rho} = \langle \alpha(\omega) | \int d\omega' \hat{a}^\dagger(\omega') \hat{a}(\omega') | \alpha(\omega) \rangle \quad (77)$$

From Eq. (76) we find that in the case of a finite density of states at $\omega = 0$ we have $\tilde{\rho} \rightarrow \infty$ and consequently the tunneling elements go to zero. This manifests dephasing due to low-frequency noise. As this is a zero-frequency effect, the amplitudes can be interpreted to have finite momentary values, but vanishing long-time averages. It can also be shown that the factor $\exp(-\tilde{\rho})$ is a continuous-mode generalization of the renormalization factor $\exp(-\rho)$ in the $P(E)$ -function of a single-mode environment [2].

2. Multi-photon processes

Let us consider now multi-photon production, i.e., the case $n \geq 2$ in Eq. (63). To evaluate this in the first order of I_c , we insert the displacement operator once in the n possible out-operators in expression

$$T^{1 \rightarrow n} = \left\langle [\hat{a}_{\text{out}}(\omega_1) \dots \hat{a}_{\text{out}}(\omega_n)] \hat{a}_{\text{in}}^\dagger(\omega) \right\rangle.$$

We find that the result is non-zero only if the leading-order solution for the out-field is inserted to operators of frequencies ω_{n-1} or ω_n . We now write the leading-order result in the form

$$T_1^{1 \rightarrow n} = \mathcal{T}^{1 \rightarrow n} + \sum_{i=1}^n t_i^{1 \rightarrow n}, \quad (78)$$

where the first part has the form

$$\begin{aligned} \mathcal{T}^{1 \rightarrow n} &= \frac{I_c}{2e} \pi e^{-\tilde{\rho}/2} \delta(\omega + \omega_J - \omega_1 - \dots - \omega_n) \\ &\times \alpha^*(\omega) \alpha^*(\omega_1) \dots \alpha^*(\omega_n), \end{aligned} \quad (79)$$

which describes n -photon emission with energy conservation, $\omega + \omega_J = \omega_1 + \dots + \omega_n$: The electrostatic energy released in a Cooper-pair tunneling is absorbed by the ensemble of photons. Many different scattering processes are possible, depending on distributions $\alpha(\omega_i)$, but the individual frequencies always sum up to $\omega + \omega_J$.

We also get n additional terms of the form

$$\begin{aligned} t_1^{1 \rightarrow n} &= \frac{I_c}{2e} \pi e^{-\tilde{\rho}/2} \delta(\omega - \omega_1) \delta(\omega_J - \omega_2 - \omega_3 - \dots - \omega_n) \\ &\times \frac{\alpha^*(\omega_1)}{\alpha(\omega_1)} \alpha^*(\omega_2) \alpha^*(\omega_3) \dots \alpha^*(\omega_n). \end{aligned} \quad (80)$$

These additional terms manifest an elastic reflection of the input photon of frequency ω to mode ω_i . The rest of the photons appear due to direct emission, i.e., emis-

sion triggered by vacuum fluctuations. Furthermore, if the background emission is unwanted, it is possible to reduce it by engineering the tunnel impedance, $\text{Re}[Z_t(\omega)] = Z_0 |A(\omega)|^2 \propto |\alpha(\omega)|^2$, so that it has a small value at frequencies that need to be used in unwanted processes [49].

Consider finally scattering amplitudes between general photon-number states. Assuming an m -photon input, we get for the term describing the full conversion to n -photon output

$$\begin{aligned} \mathcal{T}^{m \rightarrow n} &= \frac{I_c}{2e} \pi e^{-\tilde{\rho}/2} \\ &\times \alpha^*(\omega'_1) \dots \alpha^*(\omega'_m) \alpha^*(\omega_1) \dots \alpha^*(\omega_n) \\ &\times \delta(\omega'_1 + \dots + \omega'_m + \omega_J - \omega_1 - \dots - \omega_n), \end{aligned} \quad (81)$$

where the incoming frequencies are now labeled as $\omega'_1 \dots \omega'_m$. The rest of obtained terms (not listed above) describe a conversion of only part of the incoming photons, and emission of background photons triggered by vacuum fluctuations, similarly as above.

VI. CONCLUSIONS AND DISCUSSION

In conclusion, we have analyzed how incoming microwaves of different forms scatter by a DC-voltage biased Josephson junction. Scattering effects for general circuits can be described in terms of the $P(E)$ function and expectation values of a displacement operator. The main practical findings were that thermal and coherent radiation can be absorbed and amplified in a circuit with a resonance frequency, and that coherent radiation can be converted into two-mode squeezed microwaves. Furthermore, the non-linear interaction at the junction allows for engineering, in principle, any photon multiplication and multi-photon absorption processes, with appropriate tailoring of the impedance as seen by the Josephson junction. Such systems then offer new ways to process quantum microwaves on-chip.

The analysis presented in this article was made in the perturbative regime, which provides a simple and intuitive working environment for understanding inelastic Cooper-pair tunneling in general microwave circuits. In the strict validity region of the perturbative solution, the incoming radiation is mostly reflected, rather than scattered to different modes. Alternative models applicable in the opposite limit [25, 26, 49], non-perturbative methods through self-consistent expansions [58], and direct calculations of relevant higher-order contributions [27, 38] have also been established.

A future interest is a deeper understanding of quantum information created by quantum transport, and its engineering by microwave circuit design. In particular, the created radiation can consist of high-photon-number bundles or show very strong photon anti-bunching. The radiation can be tailored to be broadband and fast, or concentrated to narrow resonance frequencies. It can also

carry information of the underlying quantum transport. Novel methods and ideas for characterization and detection of quantum information in such forms of microwave light are then of great interest theoretically and experimentally.

Acknowledgments

The authors thank M. Hofheinz, D. Hazra, A. Grimm, F. Blanchet, R. Albert, S. Jebari, F. Portier, A. Peu-

geot, I. Moukharski, P. Joyez, C. Altimiras, D. Vion, B. Kubala, S. Dambach, J. Ankerhold, M. Fogelström, and G. Johansson for fruitful discussions at different stages of this project. This work has been supported by the DFG Grant No. MA 6334/3-1.

-
- [1] M. H. Devoret, D. Esteve, H. Grabert, G.-L. Ingold, H. Pothier, and C. Urbina, Phys. Rev. Lett. **64**, 1824 (1990), URL <http://dx.doi.org/10.1103/PhysRevLett.64.1824>.
 - [2] G.-L. Ingold and Y. V. Nazarov, *Single Charge Tunneling: Coulomb Blockade Phenomena in Nanostructures* (Plenum, New York, 1992).
 - [3] T. Holst, D. Esteve, C. Urbina, and M. H. Devoret, Phys. Rev. Lett. **73**, 3455 (1994), URL <http://dx.doi.org/10.1103/physrevlett.73.3455>.
 - [4] J. Leppäkangas, E. Thuneberg, R. Lindell, and P. Hakonen, Phys. Rev. B **74**, 054504 (2006), URL <http://dx.doi.org/10.1103/physrevb.74.054504>.
 - [5] Y. A. Pashkin, H. Im, J. Leppäkangas, T. F. Li, O. Astafiev, A. A. Abdumalikov Jr., E. Thuneberg, and J. S. Tsai, Phys. Rev. B **83**, 020502(R) (2011), URL <http://dx.doi.org/10.1103/physrevb.83.020502>.
 - [6] A. Cottet, T. Kontos, and B. Doucot, Phys. Rev. B **91**, 205417 (2015), URL <http://dx.doi.org/10.1103/physrevb.91.205417>.
 - [7] C. Altimiras, F. Portier, and P. Joyez, Phys. Rev. X **6**, 031002 (2016), URL <http://dx.doi.org/10.1103/physrevx.6.031002>.
 - [8] M. Hofheinz, F. Portier, Q. Baudouin, P. Joyez, D. Vion, P. Bertet, P. Roche, and D. Esteve, Phys. Rev. Lett. **106**, 217005 (2011), URL <http://dx.doi.org/10.1103/physrevlett.106.217005>.
 - [9] G. Gasse, C. Lupien, and B. Reulet, Phys. Rev. Lett. **111**, 136601 (2013), URL <http://dx.doi.org/10.1103/physrevlett.111.136601>.
 - [10] J.-C. Forgues, C. Lupien, and B. Reulet, Phys. Rev. Lett. **113**, 043602 (2014), URL <http://dx.doi.org/10.1103/physrevlett.113.043602>.
 - [11] J.-C. Forgues, C. Lupien, and B. Reulet, Phys. Rev. Lett. **114**, 130403 (2015), URL <http://dx.doi.org/10.1103/physrevlett.114.130403>.
 - [12] C. Altimiras, O. Parlavecchio, P. Joyez, D. Vion, P. Roche, D. Esteve, and F. Portier, Phys. Rev. Lett. **112**, 236803 (2014), URL <http://dx.doi.org/10.1103/physrevlett.112.236803>.
 - [13] F. Chen, J. Li, A. D. Armour, E. Brahim, J. Stettenheim, A. J. Sirois, R. W. Simmonds, M. P. Blencowe, and A. J. Rimberg, Phys. Rev. B **90**, 020506(R) (2014), URL <http://dx.doi.org/10.1103/physrevb.90.020506>.
 - [14] Y.-Y. Liu, J. Stehlik, C. Eichler, M. J. Gullans, J. M. Taylor, and J. R. Petta, Science **347**, 285 (2015), URL <http://dx.doi.org/10.1126/science.aaa2501>.
 - [15] O.-P. Saira, M. Zgirski, K. L. Viisanen, D. S. Golubev, and J. P. Pekola, Phys. Rev. Applied **6**, 024005 (2016), URL <http://dx.doi.org/10.1103/physrevapplied.6.024005>.
 - [16] S. Masuda, K. Y. Tan, M. Partanen, R. E. Lake, J. Govenius, M. Silveri, H. Grabert, and M. Möttönen, Sci. Rep. **8**, 3966 (2018), URL <http://dx.doi.org/10.1038/s41598-018-21772-5>.
 - [17] M. C. Cassidy, A. Bruno, S. Rubbert, M. Irfan, J. Kammhuber, R. N. Schouten, A. R. Akhmerov, and L. P. Kouwenhoven, Science **355**, 939 (2017), URL <http://dx.doi.org/10.1126/science.aah6640>.
 - [18] M. Westig, B. Kubala, O. Parlavecchio, Y. Mukharsky, C. Altimiras, P. Joyez, D. Vion, P. Roche, M. Hofheinz, D. Esteve, et al., Phys. Rev. Lett. **119**, 137001 (2017), URL <https://doi.org/10.1103/PhysRevLett.119.137001>.
 - [19] J. Sarkar, C. Padurariu, A. Puska, D. Golubev, and P. J. Hakonen, arXiv:1706.02895 (2017), URL <https://arxiv.org/abs/1706.02895>.
 - [20] S. Jebari, F. Blanchet, A. Grimm, D. Hazra, R. Albert, P. Joyez, D. Vion, D. Estève, F. Portier, and M. Hofheinz, Nature Electronics **1**, 223 (2018), URL <https://doi.org/10.1038/s41928-018-0055-7>.
 - [21] A. Grimm, F. Blanchet, R. Albert, J. Leppäkangas, S. Jebari, D. Hazra, F. Gustavo, J.-L. Thomassin, E. Dupont-Ferrier, F. Portier, et al., arXiv:1804.10596 (2018), URL <https://arxiv.org/abs/1804.10596>.
 - [22] C. W. J. Beenakker and H. Schomerus, Phys. Rev. Lett. **86**, 700 (2001), URL <http://dx.doi.org/10.1103/physrevlett.86.700>.
 - [23] M. Marthaler, J. Leppäkangas, and J. H. Cole, Phys. Rev. B **83**, 180505(R) (2011), URL <http://dx.doi.org/10.1103/physrevb.83.180505>.
 - [24] J. Leppäkangas, G. Johansson, M. Marthaler, and M. Fogelström, Phys. Rev. Lett. **110**, 267004 (2013), URL <http://dx.doi.org/10.1103/physrevlett.110.267004>.
 - [25] A. D. Armour, M. P. Blencowe, E. Brahim, and A. J. Rimberg, Phys. Rev. Lett. **111**, 247001 (2013), URL <http://dx.doi.org/10.1103/physrevlett.111.247001>.
 - [26] V. Gramich, B. Kubala, S. Rohrer, and J. Ankerhold, Phys. Rev. Lett. **111**, 247002 (2013), URL <http://dx.doi.org/10.1103/physrevlett.111.247002>.
 - [27] F. Xu, C. Holmqvist, and W. Belzig, Phys. Rev. Lett. **113**, 066801 (2014), URL <http://dx.doi.org/10.1103/>

- PhysRevLett. **113**.066801.
- [28] J.-R. Souquet, M. J. Woolley, J. Gabelli, P. Simon, and A. A. Clerk, Nat. Commun. **5**, 5562 (2014), URL <http://dx.doi.org/10.1038/ncomms5562>.
- [29] N. Lambert, F. Nori, and C. Flindt, Phys. Rev. Lett. **115**, 216803 (2015), URL <http://dx.doi.org/10.1103/physrevlett.115.216803>.
- [30] F. Hassler and D. Otten, Phys. Rev. B **92**, 195417 (2015), URL <http://dx.doi.org/10.1103/physrevb.92.195417>.
- [31] M. Trif and P. Simon, Phys. Rev. B **92**, 014503 (2015), URL <http://dx.doi.org/10.1103/physrevb.92.014503>.
- [32] A. L. Grimsmo, F. Qassemi, B. Reulet, and A. Blais, Phys. Rev. Lett. **116**, 043602 (2016), URL <http://dx.doi.org/10.1103/PhysRevLett.116.043602>.
- [33] S. Dambach, B. Kubala, V. Gramich, and J. Ankerhold, Phys. Rev. B **92**, 054508 (2015), URL <http://dx.doi.org/10.1103/physrevb.92.054508>.
- [34] J. Leppäkangas, M. Fogelström, A. Grimm, M. Hofheinz, M. Marthaler, and G. Johansson, Phys. Rev. Lett. **115**, 027004 (2015), URL <http://dx.doi.org/10.1103/physrevlett.115.027004>.
- [35] U. C. Mendes and C. Mora, New J. Phys. **17**, 113014 (2015), URL <http://dx.doi.org/10.1088/1367-2630/17/11/113014>.
- [36] J.-R. Souquet and A. A. Clerk, Phys. Rev. A **93**, 060301(R) (2016), URL <http://dx.doi.org/10.1103/physreva.93.060301>.
- [37] C. Mora, C. Altimiras, P. Joyez, and F. Portier, Phys. Rev. B **95**, 125311 (2017), URL <http://dx.doi.org/10.1103/physrevb.95.125311>.
- [38] J. Leppäkangas, M. Fogelström, M. Marthaler, and G. Johansson, Phys. Rev. B **93**, 014506 (2016), URL <http://dx.doi.org/10.1103/physrevb.93.014506>.
- [39] S. Dambach, B. Kubala, and J. Ankerhold, New J. Phys. **19**, 023027 (2017), URL <http://dx.doi.org/10.1088/1367-2630/aa5bb6>.
- [40] M. Koppenhöfer, J. Leppäkangas, and M. Marthaler, Phys. Rev. B **95**, 134515 (2017), URL <http://dx.doi.org/10.1103/physrevb.95.134515>.
- [41] U. C. Mendes, P. Joyez, B. Reulet, A. Blais, F. Portier, C. Mora, and C. Altimiras, arXiv:1802.07323 (2018), URL <https://arxiv.org/abs/1802.07323>.
- [42] S. H. Simon and N. R. Cooper, Phys. Rev. Lett. **121**, 027004 (2018), URL <https://doi.org/10.1103/PhysRevLett.121.027004>.
- [43] J. Leppäkangas, G. Johansson, M. Marthaler, and M. Fogelström, New J. Phys. **16**, 015015 (2014), URL <http://dx.doi.org/10.1088/1367-2630/16/1/015015>.
- [44] R. Loudon, *The Quantum Theory of Light* (Oxford University Press, New York, 2010).
- [45] C. Gardiner and P. Zoller, *Quantum Noise* (Springer, Berlin, 2004).
- [46] H. Grabert, G.-L. Ingold, and B. Paul, Europhys. Lett. **44**, 360 (1998), URL <http://dx.doi.org/10.1209/epl/i1998-00480-8>.
- [47] M. Frey and H. Grabert, Phys. Rev. B **94**, 045429 (2016), URL <http://dx.doi.org/10.1103/physrevb.94.045429>.
- [48] M. Silveri, H. Grabert, S. Masuda, K. Y. Tan, and M. Möttönen, Phys. Rev. B **96**, 094524 (2017), URL <http://dx.doi.org/10.1103/physrevb.96.094524>.
- [49] J. Leppäkangas, M. Marthaler, D. Hazra, S. Jebari, R. Albert, F. Blanchet, G. Johansson, and M. Hofheinz, Phys. Rev. A **97**, 013855 (2018), URL <https://doi.org/10.1103/PhysRevA.97.013855>.
- [50] D. F. Walls and G. Milburn, *Quantum Optics* (Springer, Berlin, 2008).
- [51] C. Eichler, D. Bozyigit, C. Lang, M. Baur, L. Steffen, J. M. Fink, S. Filipp, and A. Wallraff, Phys. Rev. Lett. **107**, 113601 (2011), URL <http://dx.doi.org/10.1103/physrevlett.107.113601>.
- [52] P. D. Nation, J. R. Johansson, M. P. Blencowe, and F. Nori, Rev. Mod. Phys. **84**, 1 (2012), URL <https://doi.org/10.1103/RevModPhys.84.1>.
- [53] J. R. Johansson, G. Johansson, C. M. Wilson, P. Delsing, and F. Nori, Phys. Rev. A **87**, 043804 (2013), URL <http://dx.doi.org/10.1103/physreva.87.043804>.
- [54] C. M. Wilson, G. Johansson, A. Pourkabirian, M. Simoen, J. R. Johansson, T. Duty, F. Nori, and P. Delsing, Nature **376** (2011), URL <http://dx.doi.org/10.1038/nature10561>.
- [55] P. Lähdenmäki, G. S. Paraoanu, J. Hassel, and P. J. Hakonen, Proc. Natl. Acad. Sci. U.S.A **110**, 4234 (2013), URL <https://doi.org/10.1073/pnas.1212705110>.
- [56] B. H. Schneider, A. Bengtsson, I. M. Svensson, T. Aref, G. Johansson, J. Bylander, and P. Delsing, arXiv:1802.05529 (2018), URL <https://arxiv.org/abs/1802.05529>.
- [57] A. Miranowicz, M. Bartkowiak, X. Wang, Y. X. Liu, and F. Nori, Phys. Rev. A **82**, 013824 (2010), URL <http://dx.doi.org/10.1103/physreva.82.013824>.
- [58] M. Marthaler and J. Leppäkangas, Phys. Rev. B **94**, 144301 (2016), URL <http://dx.doi.org/10.1103/physrevb.94.144301>.

Appendix A: Photon flux density

The evaluation of correlators such as $\langle a^\dagger(\omega)a(\omega') \rangle$ follows guidelines given in Refs. [38, 43]. The technical difference is the presence of a coherent input at ω_0 , inducing sidebands and finite contributions also for $\omega \neq \omega'$.

1. Flux outside the drive frequency ω_0

Consider now the evaluation of contribution $\int_0^\infty d\omega' \langle \hat{a}_1^\dagger(\omega)\hat{a}_1(\omega') \rangle$, where the leading-order solution for the out-field operator $\hat{a}_{\text{out}}(\omega)$ to be inserted here is

$$\begin{aligned}
\hat{a}_1(\omega) &= iI_c \sqrt{\frac{Z_0}{\hbar\omega\pi}} A(\omega) \int_{-\infty}^{\infty} dt e^{i\omega t} \sin[\omega_J t + a \cos \omega_0 t - \hat{\phi}_0(t)] \\
&= iI_c \sqrt{\frac{Z_0}{\hbar\omega\pi}} A(\omega) \int_{-\infty}^{\infty} dt e^{i\omega t} \left[\frac{1}{2i} e^{i\omega_J t - i\hat{\phi}_0(t)} \sum_{n=-\infty}^{\infty} i^n J_n(a) e^{in\omega_0 t} + \text{H.c.} \right].
\end{aligned} \tag{A1}$$

This accounts for the incoming coherent field as phase $a(t) = a \cos \omega_0 t$ (we use here a different front sign as in the main text). In the second line we have inserted an expansion in terms of Bessel functions J_n ,

$$e^{ia \cos \omega_0 t} = \sum_{n=-\infty}^{\infty} i^n J_n(a) e^{in\omega_0 t}. \tag{A2}$$

We get for forward Cooper-pair tunneling

$$\begin{aligned}
\langle \hat{a}_1^\dagger(\omega) \hat{a}_1(\omega') \rangle &= \int_{-\infty}^{\infty} dt \int_{-\infty}^{\infty} dt' e^{-i(\omega - \omega_J)t + i(\omega' - \omega_J)t'} \\
&\times (i)^{n-m} \sum_{n=-\infty}^{\infty} \sum_{m=-\infty}^{\infty} e^{-im\omega_0 t'} e^{in\omega_0 t} \langle e^{-i\hat{\phi}_0(t)} e^{i\hat{\phi}_0(t')} \rangle \\
&\times J_m(a) J_n(a).
\end{aligned} \tag{A3}$$

In the next step we do a change of integration variables

$$\begin{aligned}
x &= t - t' & t &= \frac{x}{2} + y \\
y &= \frac{t + t'}{2} & t' &= y - \frac{x}{2}.
\end{aligned}$$

The integration over the variable y leads to the energy-conservation factor

$$2\pi \delta[\omega - \omega' - (n - m)\omega_0] e^{ix(\omega_J - \omega + n\omega_0)}. \tag{A4}$$

We choose $n = m$, which leads to (including both Cooper-pair tunneling directions)

$$\begin{aligned}
\langle \hat{a}_1^\dagger(\omega) \hat{a}_1(\omega') \rangle &= \sum_{\pm} \sum_{n=-\infty}^{\infty} \frac{\pi I_c^2 Z_0 |A(\omega)|^2}{\omega} \\
&\times P[\hbar(\pm\omega_J + n\omega_0 - \omega)] |J_n(a)|^2 \delta(\omega - \omega').
\end{aligned} \tag{A5}$$

This contribution describes emission to frequency ω .

The terms $n \neq m$ give non-diagonal contributions in frequency ($\omega \neq \omega'$). These terms describe a beating effect in $f(\omega) = \int d\omega' \langle \hat{a}^\dagger(\omega) a(\omega') \rangle / 2\pi$, but do not contribute to long-time averages.

Additional flux-contributions originating in the second-order solution $\hat{a}_2^\dagger(\omega)$ (given below) appear through terms $\langle \hat{a}_2^\dagger(\omega) \hat{a}_0(\omega') \rangle + \langle \hat{a}_0^\dagger(\omega) \hat{a}_2(\omega') \rangle$ also

appear. When $a = 0$, a direct calculation [43] gives

$$\begin{aligned}
&\int d\omega' \frac{1}{2\pi} \left[\langle \hat{a}_2^\dagger(\omega) \hat{a}_0(\omega') \rangle + \langle \hat{a}_0^\dagger(\omega) \hat{a}_2(\omega') \rangle \right] \\
&= \frac{1}{e^{\beta\hbar\omega} - 1} \frac{I_c^2 Z_0 |A(\omega)|^2}{2\omega} \\
&\times \sum_{\pm} [P(\pm\hbar\omega_J - \hbar\omega) - P(\pm\hbar\omega_J + \hbar\omega)].
\end{aligned} \tag{A6}$$

The terms proportional to $P(\pm\hbar\omega_J - \hbar\omega)$ are interpreted to describe emission to frequency ω and the terms proportional to $P(\pm\hbar\omega_J + \hbar\omega)$ absorption from frequency ω .

Similarly as above, the presence of a coherent input of amplitude a at frequency ω_0 generalizes this expression to

$$\begin{aligned}
&\int d\omega' \frac{1}{2\pi} \left[\langle \hat{a}_2^\dagger(\omega) \hat{a}_0(\omega') \rangle + \langle \hat{a}_0^\dagger(\omega) \hat{a}_2(\omega') \rangle \right] \\
&= \sum_{n=-\infty}^{\infty} |J_n(a)|^2 \frac{1}{e^{\beta\hbar\omega} - 1} \frac{I_c^2 Z_0 |A(\omega)|^2}{2\omega} \\
&\times \sum_{\pm} [P(\pm\hbar\omega_J + n\hbar\omega_0 - \hbar\omega) - P(\pm\hbar\omega_J + n\hbar\omega_0 + \hbar\omega)].
\end{aligned} \tag{A7}$$

Again, the terms proportional to $P(\pm\hbar\omega_J + n\hbar\omega_0 - \hbar\omega)$ are interpreted to describe emission to frequency ω and the terms proportional to $P(\pm\hbar\omega_J + n\hbar\omega_0 + \hbar\omega)$ absorption from frequency ω . Using the relation

$$1 + \frac{1}{e^{\beta\hbar\omega} - 1} = \frac{1}{1 - e^{-\beta\hbar\omega}} \tag{A8}$$

we can combine the emission terms with contributions from Eq. (A5) to get the first contribution on the right-hand side of Eq. (38).

2. Flux at the drive frequency ω_0

A striking feature of the calculation is the emergence of additional delta-function terms centered at ω_0 . These terms describe flux changes of drive photons only, due to photon absorption and induced emission. We evaluate first

$$\langle \hat{a}_0^\dagger(\omega') \hat{a}_2(\omega) \rangle = \frac{\alpha^* A^*(\omega')}{A(\omega')} \delta(\omega' - \omega_0) \langle \hat{a}_2(\omega) \rangle. \tag{A9}$$

Here we have used the fact that an incoming coherent state is a left-hand side eigenstate of operator $\hat{a}_0^\dagger = (A^*/A)\hat{a}_{\text{in}}^\dagger$. After this the ensemble average is subjected to operator $\hat{a}_2(\omega)$ only. We note that if operating with \hat{a}_0^\dagger to the thermal background instead (at lower frequen-

cies), we would finally get Eq. (A7). As before, the phase of α is assumed to be the opposite of A .

The second-order solution for the out field has the form [38]

$$\hat{a}_2(\omega) = \frac{E_J I_c}{\hbar} \sqrt{\frac{Z_0}{\pi \hbar \omega}} A(\omega) \int_{-\infty}^{\infty} dt \int_{-\infty}^t dt' e^{i\omega t} \{ \cos[\omega_J t' + a \cos \omega_0 t' - \phi_0(t')] \sin[\omega_J t + a \cos \omega_0 t - \phi_0(t)] - \text{H.c.} \} . \quad (\text{A10})$$

This again accounts for the incoming coherent field as phase $a(t) = a \cos \omega_0 t$. The expansion of the sinusoidal

functions leads to two terms

$$\frac{E_J I_c}{\hbar} \sqrt{\frac{Z_0}{\pi \hbar \omega}} A(\omega) \int_{-\infty}^{\infty} dt \int_{-\infty}^t dt' e^{i\omega t} \left[-\frac{1}{4i} e^{J(t'-t)} e^{i\omega_J(t'-t)+a(t')-a(t)} + \frac{1}{4i} e^{J(t'-t)} e^{i\omega_J(t-t')+a(t)-a(t')} \right] . \quad (\text{A11})$$

and

$$\frac{E_J I_c}{\hbar} \sqrt{\frac{Z_0}{\pi \hbar \omega}} A(\omega) \int_{-\infty}^{\infty} dt \int_{-\infty}^t dt' e^{i\omega t} \left[-\frac{1}{4i} e^{J(t-t')} e^{i\omega_J(t-t')+a(t)-a(t')} + \frac{1}{4i} e^{J(t-t')} e^{i\omega_J(t'-t)+a(t')-a(t)} \right] . \quad (\text{A12})$$

To find frequency correlations that sum to ω_0 , the expansion in terms of the Bessel functions have to be restricted to specific nearby numbers, i.e., we expand

This expansion transforms the two contributions to

$$\begin{aligned} e^{-a(t)+a(t')} &= \sum_n -i J_{n+1}(a) J_n(a) e^{-(n+1)i\omega_0 t} e^{ni\omega_0 t'} \\ &= \sum_n -i J_{n+1}(a) J_n(a) e^{ni\omega_0(t'-t)} e^{-i\omega_0 t} \end{aligned} \quad (\text{A13})$$

$$\begin{aligned} e^{a(t)-a(t')} &= \sum_n -i J_{n-1}(a) J_n(a) e^{(n-1)i\omega_0 t} e^{-ni\omega_0 t'} \\ &= -i J_{n-1}(a) J_n(a) e^{ni\omega_0(t-t')} e^{-i\omega_0 t} . \end{aligned} \quad (\text{A14})$$

$$\begin{aligned} &\frac{1}{4} \frac{E_J I_c}{\hbar} \sqrt{\frac{Z_0}{\pi \hbar \omega}} A(\omega) \int_{-\infty}^{\infty} dt \int_{-\infty}^t dt' e^{i\omega t} \\ &\times \left[\sum_n J_{n+1}(a) J_n(a) e^{J(t'-t)} e^{i\omega_J(t'-t)+ni\omega_0(t'-t)} e^{-i\omega_0 t} - \sum_n J_{n-1}(a) J_n(a) e^{J(t'-t)} e^{-i\omega_J(t'-t)-ni\omega_0(t'-t)} e^{-i\omega_0 t} \right] . \end{aligned} \quad (\text{A15})$$

and

$$\begin{aligned} & \frac{1}{4} \frac{E_J I_c}{\hbar} \sqrt{\frac{Z_0}{\pi \hbar \omega}} A(\omega) \int_{-\infty}^{\infty} dt \int_{-\infty}^t dt' e^{i\omega t} \\ & \times \left[\sum_n J_{n-1}(a) J_n(a) e^{J(-t'+t)} e^{i\omega_J(-t'+t) + n i \omega_0(-t'+t)} e^{-i\omega_0 t} - \sum_n J_{n+1}(a) J_n(a) e^{J(-t'+t)} e^{-i\omega_J(-t'+t) - n i \omega_0(-t'+t)} e^{-i\omega_0 t} \right]. \end{aligned} \quad (\text{A16})$$

We do a change of variables $x = t' - t$ and $y = (t' + t)/2$. Unrestricted integration over y can be immediately performed giving $2\pi\delta(\omega - \omega_0)$. Combining the first term of Eq. (A15) and the second term of Eq. (A16) we get contributions of type

$$\begin{aligned} & \int_{-\infty}^0 dx e^{i\bar{\omega}x} [e^{J(x)} - e^{J(-x)}] = 2i \int_{-\infty}^0 dx \text{Im}[e^{J(x)}] e^{i\bar{\omega}x} \\ & = 2i \int_{-\infty}^0 dx \text{Im}[e^{J(x)}] (\cos \bar{\omega}x + i \sin \bar{\omega}x) \\ & = i \int_{-\infty}^{\infty} dx \text{Im}[e^{J(x)}] \text{Sgn}(x) \cos \bar{\omega}x \\ & - \int_{-\infty}^{\infty} dx \text{Im}[e^{J(x)}] \sin \bar{\omega}x, \end{aligned} \quad (\text{A17})$$

where $\bar{\omega} = \omega_J + n\omega_0$. In the last form, the first term is

purely imaginary, as the other term is purely real. It will be only the real part that survives in the final expression, after summation also over $\langle \hat{a}_2^\dagger(\omega) \hat{a}_0 \rangle$. This means that such summation contributes as

$$\begin{aligned} & -2 \int_{-\infty}^{\infty} dx \text{Im}[e^{J(x)}] \sin \bar{\omega}x \\ & = -2 \int_{-\infty}^{\infty} dx \frac{1}{2i} [e^{J(x)} - e^{J(-x)}] \frac{1}{2i} [e^{i\bar{\omega}x} - e^{-i\bar{\omega}x}] \\ & = 2\pi\hbar [P(\hbar\bar{\omega}) - P(-\hbar\bar{\omega})]. \end{aligned} \quad (\text{A18})$$

The second term of Eq. (A15) and the first term of Eq. (A16) contribute similarly, with $\bar{\omega} = -\omega_J - n\omega_0$ and an overall minus-sign.

We notice now that all contributions sum as

$$2\pi\delta(\omega - \omega_0) \frac{1}{4} \frac{E_J I_c}{\hbar} \sqrt{\frac{Z_0}{\pi \hbar \omega}} A(\omega) \left[\sum_n J_{n+1}(a) J_n(a) + \sum_n J_{n-1}(a) J_n(a) \right] 2\pi\hbar [P(\hbar\omega_J + n\hbar\omega_0) - P(-\hbar\omega_J - n\hbar\omega_0)]. \quad (\text{A19})$$

For Bessel functions $J_{n+1}(x) + J_{n-1}(x) = (2n/x)J_n(x)$, which implies

$$J_n(x)J_{n+1}(x) + J_n(x)J_{n-1}(x) = \frac{2n}{x} J_n^2(x). \quad (\text{A20})$$

This transforms contribution (A19) to

$$\begin{aligned} & 2\pi\delta(\omega - \omega_0) \frac{1}{4} \frac{E_J I_c}{\hbar} \sqrt{\frac{Z_0}{\pi \hbar \omega}} A(\omega) \frac{2n}{a} \\ & \times \sum_n |J_n(a)|^2 2\pi\hbar [P(\hbar\omega_J + n\hbar\omega_0) - P(-\hbar\omega_J - n\hbar\omega_0)]. \end{aligned} \quad (\text{A21})$$

Multiplying by $\alpha^* A^*(\omega')/[A(\omega')]\delta(\omega' - \omega_0)$, using the connection $\sqrt{8Z_0/\omega_0 R_Q} \alpha A(\omega_0) = -a$, and integrating over all frequencies, we get the photon-flux change at the drive mode

$$-\frac{I_c^2 R_Q}{4} \sum_{n=-\infty}^{\infty} |J_n(a)|^2 [nP[\hbar(n\omega_0 + \omega_J)] + nP[\hbar(n\omega_0 - \omega_J)]] \quad (\text{A22})$$

Appendix B: Energy conservation

The derived equations describe microwave conversion between different frequencies mediated by inelastic Cooper-pair tunneling. For a consistent theory an energy conservation is crucial. To show this, we need to compare the power of the propagating electromagnetic radiation to the energy provided by the voltage source, IV . All quantities have to be calculated to up to the same order in the critical current I_c .

We consider first the case of thermal input (with coherent amplitude $a = 0$). The key to proving the energy conservation is the relation

$$\frac{d}{dt} \exp[J(t)] = -i \exp[J(t)] \int_0^\infty d\omega \frac{Z_0 |A(\omega)|^2}{R_Q} \left[\left(1 + \coth\left(\frac{1}{2}\beta\hbar\omega\right)\right) e^{-i\omega t} + \left(1 - \coth\left(\frac{1}{2}\beta\hbar\omega\right)\right) e^{i\omega t} \right]. \quad (\text{B1})$$

A Fourier transformation of this equation gives

$$EP(E) = \int_0^\infty \hbar d\omega \frac{Z_0 |A(\omega)|^2}{R_Q} P(E - \hbar\omega) \left[1 + \coth\left(\frac{1}{2}\beta\hbar\omega\right)\right] + \int_0^\infty \hbar d\omega \frac{Z_0 |A(\omega)|^2}{R_Q} P(E + \hbar\omega) \left[1 - \coth\left(\frac{1}{2}\beta\hbar\omega\right)\right]. \quad (\text{B2})$$

Identifying $E = 2eV$ and using the leading-order result for the forward Cooper-pair tunneling ($V > 0$),

$$I^+(V) = \frac{\pi \hbar I_c^2}{4e} P(2eV), \quad (\text{B3})$$

the work done by the voltage source gets related to the power spectral density,

$$I^+ V = \frac{I_c^2}{4} \int_0^\infty \hbar d\omega Z_0 |A(\omega)|^2 P(2eV - \hbar\omega) \left[1 + \coth\left(\frac{1}{2}\beta\hbar\omega\right)\right] + \frac{I_c^2}{4} \int_0^\infty \hbar d\omega Z_0 |A(\omega)|^2 P(2eV + \hbar\omega) \left[1 - \coth\left(\frac{1}{2}\beta\hbar\omega\right)\right]. \quad (\text{B4})$$

Relation for the backward tunneling is obtained by changing $V \rightarrow -V$. The total current is $I(V) = I^+(V) - I^-(V) = I^+(V) - I^+(-V)$. Using then relations $\coth(x/2) + 1 = 2e^x/(e^x - 1)$, $1 - \coth(x/2) = -2/(e^x - 1)$, and comparing to Eqs. (38) and (40), we get

$$IV = \int_0^\infty d\omega \hbar\omega [f_{\text{em}}(\omega) - f_{\text{abs}}(\omega)]. \quad (\text{B5})$$

This then states that the extra power in the output is the same as the work done by the external voltage source.

For a coherent state input at frequency ω_0 with amplitude $a > 0$ one can proceed similarly. The Cooper-pair current in this case is generalized to

$$I_{\omega_0}^\pm(V) = \sum_{n=-\infty}^\infty |J_n(a)|^2 \frac{\pi \hbar I_c^2}{4e} P(\pm 2eV + n\omega_0). \quad (\text{B6})$$

From Eqs. (38) and (40) we see that there are two types of contributions in the photon spectrum $f_{\text{em}}(\omega) - f_{\text{abs}}(\omega)$: (i) terms as before but with shifted energy arguments (by $n\hbar\omega_0$) and front factors $|J_n|^2$, and (ii) terms proportional to delta functions at the drive frequency ω_0 . The generalized junction current I_{ω_0} has only contributions that are similar to terms (i).

Consider now obtaining the radiation power, $\int d\omega \hbar\omega [f_{\text{em}}(\omega) - f_{\text{abs}}(\omega)]$, term by term from the power $I_{\omega_0} V$ by using the $P(E)$ -relation given by Eq. (B4) for individual contributions of $I_{\omega_0} V$. This needs multiplying of Eq. (B4) by $|J_n|^2$ and changing the energy argument as $E \leftarrow E + n\hbar\omega_0$, meaning $V \leftarrow V + n\hbar\omega_0/2e$. Summation over n gives

$$I_{\omega_0}^+ V = - \sum_{n=-\infty}^\infty n \frac{\hbar\omega_0}{2e} |J_n(a)|^2 I^+ \left(V + n \frac{\hbar\omega_0}{2e} \right) + \sum_{n=-\infty}^\infty |J_n(a)|^2 \frac{I_c^2}{4} \int_0^\infty \hbar d\omega Z_0 |A(\omega)|^2 P(2eV + n\hbar\omega_0 - \hbar\omega) \left[1 + \coth\left(\frac{1}{2}\beta\hbar\omega\right)\right] + \sum_{n=-\infty}^\infty |J_n(a)|^2 \frac{I_c^2}{4} \int_0^\infty \hbar d\omega Z_0 |A(\omega)|^2 P(2eV + n\hbar\omega_0 + \hbar\omega) \left[1 - \coth\left(\frac{1}{2}\beta\hbar\omega\right)\right]. \quad (\text{B7})$$

On the right-hand side of this equation, the integrations over frequencies match to contributions (i) in the radiation spectrum and the additional contribution proportional to $n\omega_0$ match to terms (ii) in the radiation spectrum.

Appendix C: Squeezing correlator

We evaluate here the correlator $\langle \hat{a}_{\text{out}}(\omega) \hat{a}_{\text{out}}(\omega') \rangle$ for frequencies that sum to the drive frequency, $\omega + \omega' = \omega_0$, with $\omega, \omega' > 0$. It is here only the expectation value

$\langle \hat{a}_1(\omega) \hat{a}_1(\omega') \rangle$ that gives a finite contribution, i.e., when inserting the leading order solution \hat{a}_1 into operators \hat{a}_{out} . We get two contributions

$$c \int_{-\infty}^{\infty} dt \int_{-\infty}^{\infty} dt' e^{i\omega t + i\omega' t' + i\omega_J(t-t')} e^{J(t-t')} \sum_{n=-\infty}^{\infty} \sum_{m=-\infty}^{\infty} (i)^n (-i)^m e^{in\omega_0 t} e^{-im\omega_0 t'} J_n(a) J_m(a). \quad (\text{C1})$$

and

$$c \int_{-\infty}^{\infty} dt \int_{-\infty}^{\infty} dt' e^{i\omega t + i\omega' t' - i\omega_J(t-t')} e^{J(t-t')} \sum_{n=-\infty}^{\infty} \sum_{m=-\infty}^{\infty} (-i)^n (i)^m e^{-in\omega_0 t} e^{im\omega_0 t'} J_n(a) J_m(a). \quad (\text{C2})$$

Here $c = -I_c^2 Z_0 A(\omega) A(\omega') / 4\sqrt{\omega\omega'} \hbar \pi$. We do the same change of integration variables as in Appendix A, integrate over y , and obtain the energy-conservation factor for the first term

$$2\pi\delta[\omega + \omega' + (n - m)\omega_0] e^{i(\omega + \omega_J + n\omega_0)}. \quad (\text{C3})$$

The energy-conservation factor for the second term has the form

$$2\pi\delta[\omega + \omega' - (n - m)\omega_0] e^{ix(\omega - \omega_J - n\omega_0)}. \quad (\text{C4})$$

Assuming $\omega + \omega' = \omega_0$ leads to conditions $n - m = -1$ (the first contribution) and $n - m = 1$ (the second contribution). Inserting $\int_{-\infty}^{\infty} dx e^{J(x) + iE/\hbar} = 2\pi\hbar P(E)$, the result is

$$\begin{aligned} \langle \hat{a}_1(\omega) \hat{a}_1(\omega') \rangle &= -ci4\pi^2 \hbar \delta(\omega + \omega' - \omega_0) \sum_{n=-\infty}^{\infty} P[\hbar(\omega + \omega_J + n\omega_0)] J_n(a) J_{n+1}(a) \\ &\quad - ci4\pi^2 \hbar \delta(\omega + \omega' - \omega_0) \sum_{n=-\infty}^{\infty} P[\hbar(\omega - \omega_J - n\omega_0)] J_n(a) J_{n-1}(a). \end{aligned} \quad (\text{C5})$$

Since for odd values of n the Bessel functions satisfy $J_{-n}(a) = -J_n(a)$ and for even values $J_{-n}(a) = J_n(a)$, we have

$$\begin{aligned} \langle \hat{a}_1(\omega) \hat{a}_1(\omega') \rangle &= \sum_{\pm} \mp ci4\pi^2 \hbar \delta(\omega + \omega' - \omega_0) \\ &\times \sum_{n=-\infty}^{\infty} P[\hbar(\omega \pm \omega_J + n\omega_0)] J_n(a) J_{n+1}(a). \end{aligned} \quad (\text{C6})$$